Ann. Rev. Astron. Astrophys. 1986. 24 : 377–420

MASS LOSS FROM COOL STARS[1]

A. K. Dupree

Harvard-Smithsonian Center for Astrophysics, Cambridge, Massachusetts 02138

1. INTRODUCTION

The presence and characteristics of mass loss from cool stars affect much of stellar astrophysics. Theoretical constraints and inferences, direct observations, and in situ sampling for the Sun indicate that all stars lose mass. Of ultimate interest to stellar physics are the rate of mass loss at each phase in a star's evolution and the physical mechanisms by which stars lose material to the interstellar medium. During the course of this review, it will become obvious that the detection of mass motions in, or mass loss from, a stellar atmosphere is far simpler than the evaluation of a mass-loss rate, or the derivation of a mass-loss "law" (if such a relationship even exists!). We are only slowly approaching such quantitative goals in a field that is decidedly led by observations.

Twenty-three years ago, when Weymann (1963) reviewed mass loss in the first volume of the *Annual Review of Astronomy and Astrophysics*, optical techniques were the sole means to study the mass-loss process. Most recently, powerful spectroscopic and photometric capabilities have developed through space-based observations with observatories such as *Copernicus*, IUE, HEAO-2 ("Einstein"), and IRAS. Substantial advances have occurred in photon-counting detector systems and in the achievement of high sensitivity over a broad frequency range, from radio frequencies with the VLA to high-energy phenomena with HEAO-2. These strides in technology have caused studies of mass loss to flourish and have provided new impetus for theoretical development and computer modeling activities.

This review focuses on the optical and ultraviolet spectroscopic diag-

nostics of mass loss and mass motions in cool-star atmospheres that define the constraints to theoretical models of mass loss. X-ray and ultraviolet observations demonstrate the relationship between mass loss and stellar coronae, help determine the characteristics of cool stellar winds, and permit a coherent picture of the mass-loss process in the cool half of the color-magnitude diagram (Section 3). Solar observations (Section 4) are useful in illustrating the complex nature of the magnetic field and plasma interaction in a high-gravity star, although simple extrapolations to luminous stars are not always possible. The derivation of mass-loss rates is treated in Section 5 for evolved single stars. Binary stars present certain advantages—for example, an absolute stellar scale—in obtaining mass-loss rates, although the processes themselves may be modified by the interaction of two stars. These systems are discussed in Section 6. The significance of mass loss in stellar evolution as evidenced by globular cluster populations is reviewed in Section 7. Parameterization of mass-loss rates is treated in Section 8, followed by a discussion of the constraints placed on theoretical models of mass loss by observations (Section 9). A brief list of continuing problems is itemized in Section 10.

Different aspects of stellar mass loss have been reviewed recently in these pages and elsewhere. Among the notable reviews are those on hot stars (Conti 1978); cool stars (Goldberg 1985); the theoretical basis of stellar winds (Cassinelli 1979, MacGregor 1983); envelopes around giant stars (Zuckerman 1980); and outflows, winds, and jets from young stellar objects (Lada 1985). Several conference proceedings include a number of good reviews and contributions, namely IAU Colloquium No. 59 on *Effects of Mass Loss on Stellar Evolution* (ed. C. Chiosi and R. Stalio: Reidel); the Erice Meeting on *Physical Processes in Red Giants* (ed. I. Iben Jr. and A. Renzini: Reidel); the Third Cambridge Workshop on *Cool Stars, Stellar Systems, and the Sun* (ed. S. L. Baliunas and L. Hartmann: Springer-Verlag); and *Mass Loss from Red Giants* (ed. M. Morris and B. Zuckerman: Reidel).

2. SPECTROSCOPIC DIAGNOSTICS OF MASS LOSS

For material to be lost from a star, it must attain speeds slightly in excess of the escape velocity. From a stellar surface this value is V_{esc} (km s^{-1}) = 620 $(M/R)^{1/2}$, where M and R are the mass and radius of the star in solar units. The values of V_{esc} are typically 620 km s^{-1} for a solar-type dwarf star, 310 km s^{-1} for a giant star (spectral type K0), and 110 km s^{-1} for a supergiant star (spectral type M0). Such high velocities (a "catapulted departure") are generally not observed, suggesting that the mass loss is a gentle, leisurely process. If the atmosphere is extended (values of

2 to 5 times the stellar photospheric radius are not uncommon), the velocity required for escape decreases as $R^{1/2}$, and indeed such lower velocities have been detected.

Doppler shifts of spectral features would be the most straightforward means of detecting mass motion and mass outflow. The early measurements of Adams & MacCormack (1935) of narrow blueshifted Na I, Ca H and K, and Al II absorption lines in luminous cool stars showed outward motions of ~ 5 km s^{-1} relative to the photosphere. These observations were interpreted as a slowly expanding atmosphere. Deutsch (1956) first detected the actual escape of material from a star by discovering stationary, but blueshifted, absorption features of Na I, Ca I and II, and Fe I in the optical spectrum of the G giant spectroscopic binary that is a visual companion of α Her (M5 I). These blueshifted lines indicate that material streams out at 10 km s^{-1} relative to the M star. Since the escape velocity is 6.3 km s^{-1} at the edge of the circumstellar envelope (350 R_*), Deutsch argued that the material was in fact leaving the system at a rate of $3 \times 10^{-8}\, M_\odot$ yr^{-1}.

Since this discovery, many techniques and spectral regions other than measures at optical frequencies have been used to infer mass motions or loss from a stellar atmosphere.

Fundamental to the detection of mass loss is the identification of meaningful signatures in cool stars of various temperatures and gravities. An illustration of the complexity of line and continuum formation that influences selection of diagnostics comes from the construction of detailed semiempirical models of stellar atmospheres. A solar model (Figure 1), iterated to satisfy multifrequency continuum measures and high-resolution observations of line profiles, shows that judicious selection of features (including restricted regions of line profiles) can probe very specific atmospheric levels. In a dwarf star, the Lα core represents the highest chromospheric level, followed by the Mg II core (k_3), the Ca K core (K_3), and Hα at lower levels. The separation of these various diagnostics (~ 500 km) is only a minute fraction of a stellar radius. (In the Sun, of course, higher temperatures occur beyond 2500 km, and other diagnostics become important; see Section 4.2.) Atmospheric models for low-gravity cool stars are not nearly so detailed, in part because it is only recently that quantitative measurements of many spectral features were obtained. Also, solutions of the radiative transfer equations for multilevel atoms in spherical geometries are in the early stages of development for expanding cool-star atmospheres. However, one calculation of strong chromospheric lines for a giant star with an extended expanding atmosphere demonstrates the enormous change in scale of the atmosphere (Figure 2). No longer are the classic chromospheric tracers, Ca II and Mg II, tightly coupled. The

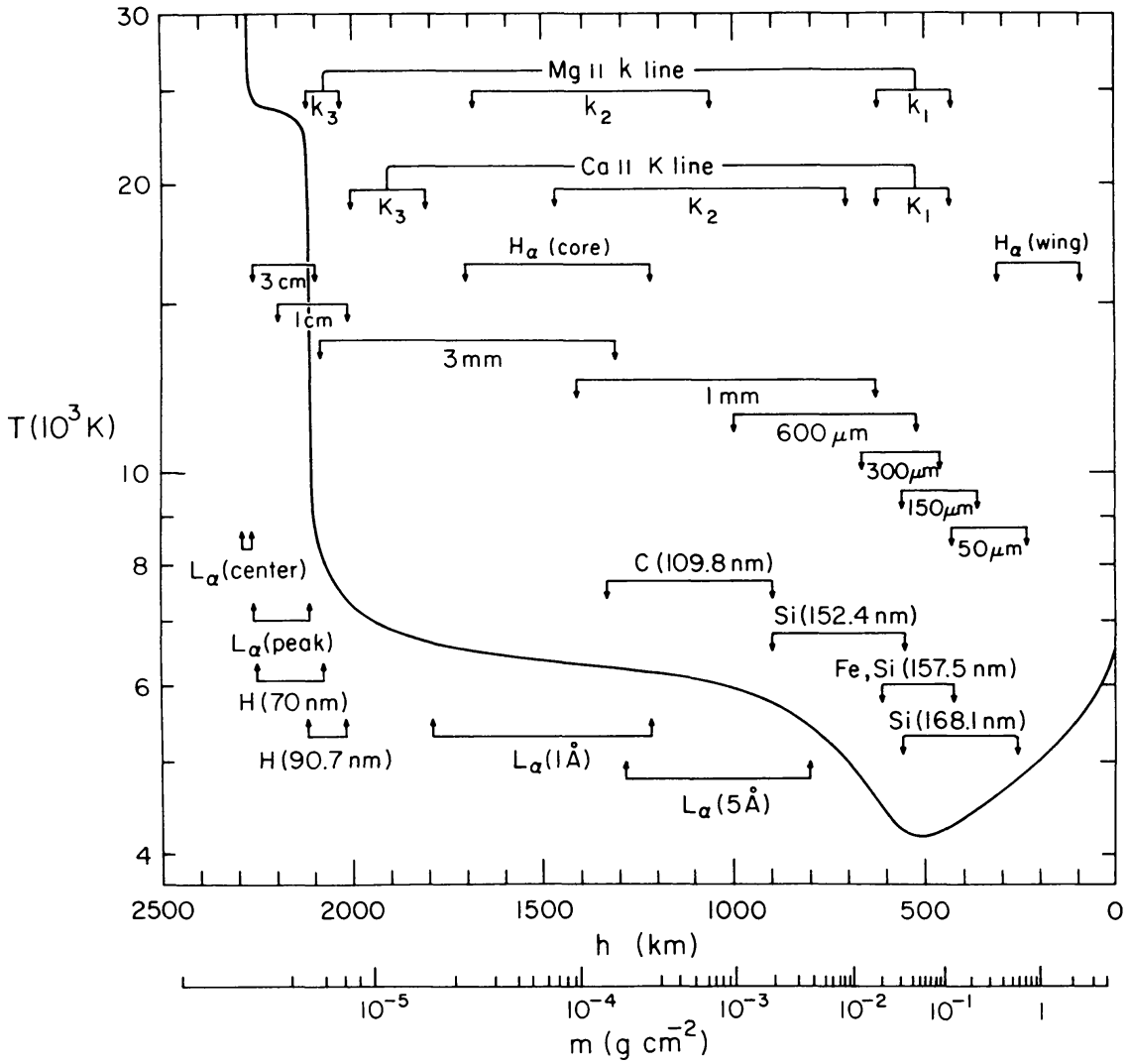

Figure 1 The temperature distribution in the average quiet solar atmosphere. This semi-empirical model was constructed from line and continuum observations at many frequencies. The approximate depth of formation of these features is noted (figure from Avrett 1981).

Mg II k line core (k_3) is separated from the calcium core (K_3) by $\sim 2\ R_*$. The Mg II k core and emission wings would be most sensitive to the farthest reaches of an extended atmosphere. The Ca K line is confined to the inner regions of the chromosphere. Such calculations demonstrate the need to choose diagnostics carefully. More extensive observations of luminous stars will undoubtedly provide additional constraints.

2.1 *Optical Signatures of Mass Loss*

2.1.1 Hα The Hα profile at λ6562.8 is an easily measurable strong absorption feature in the spectrum of cool Population I stars. In late-type dwarfs and flare stars, the line is frequently observed in emission, and in metal-deficient luminous stars, emission wings can be found.

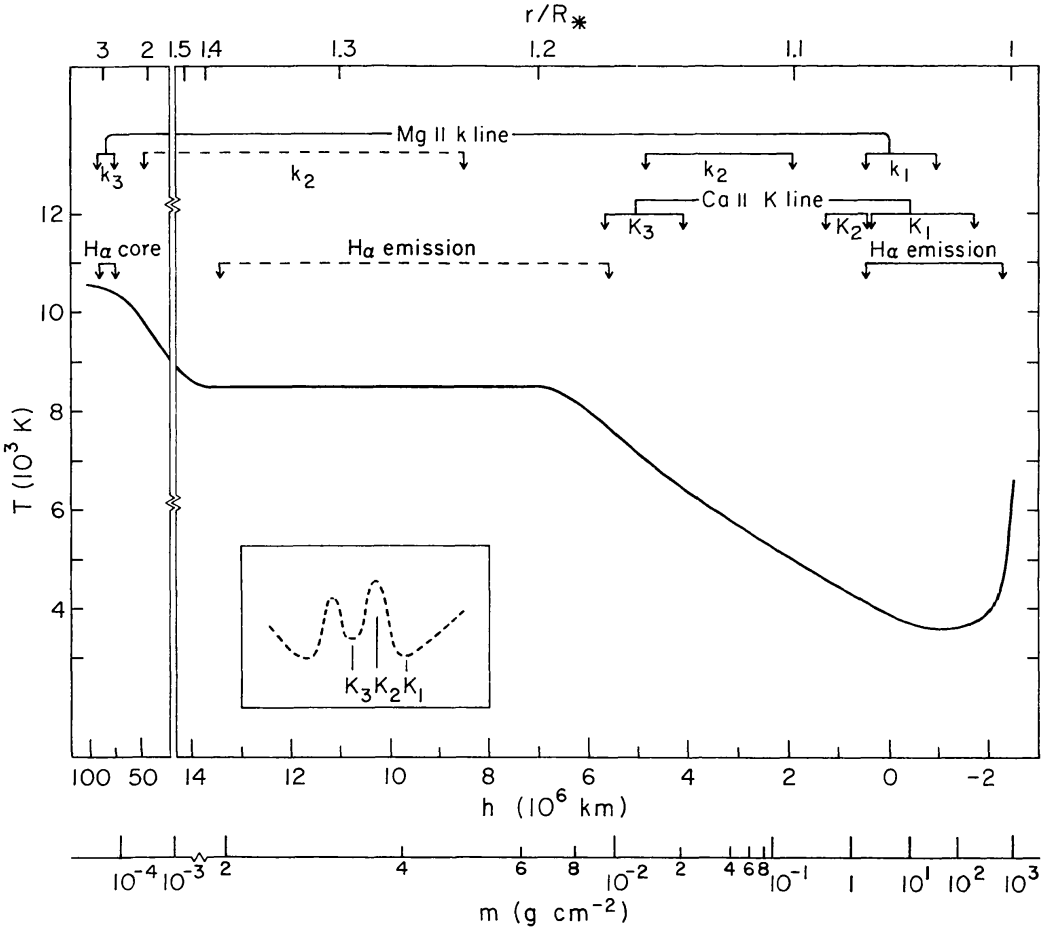

Figure 2 The temperature distribution in the extended atmosphere of a metal-deficient giant star (model 3 from Dupree et al. 1984a). This semiempirical model was constructed from observations of Hα, Ca II, and Mg II, and the approximate depth of formation (where $\tau \sim 1$) for various portions of the line profiles are shown. The broken lines indicate the depths where a substantial fraction (~30%) of a feature can be formed. Some observations (Zarro & Rodgers 1983) of Pop I stars suggest that the Hα core is formed below the Ca II (K_3) feature.

In dwarf stars, however, the Hα core is formed so deep in the chromosphere (see Figure 1) that the signature of a wind is generally not observed. However, in the lower gravities of giant and supergiant stars, the line core is formed farther out in the atmosphere, and outflows are of sufficient magnitude to be evidenced in a core asymmetry or an actual line core shift. About 50% of a sample of M giant stars (Population I) show Hα asymmetries and blueshifts (Boesgaard & Hagen 1979). In late G, K, and early M-type supergiants, Mallik (1982) measured core blueshifts of Hα ranging from -5 to -30 km s^{-1}. Metal-deficient giants show similar shifts (Section 7.2). These values may indicate a circulation pattern (although only blueshifted cores are found) or the actual beginning of an

outward acceleration. Zarro & Rodgers (1983) noted the correspondence between features of the Ca II (K) profiles and those of Hα in giants and supergiants, as well as the enhanced blueshift of Ca II (K_3) with respect to the Hα core. This suggests an ordered radial structure or motion in the atmosphere, but no quantitative modeling was carried out.

The Hα profile is difficult to interpret properly, arising as it does from an excited level of hydrogen. Its interpretation requires multilevel atomic configurations, detailed knowledge of the local radiation field for both line and continuum processes, and models with extended (moving) atmospheres. In one semiempirical model calculation for the G8 IV star λ And (Baliunas et al. 1979), the Hα profile did not provide sensitive constraints on the atmospheric structure itself, and only a few studies have focused on this diagnostic (see Mallik 1982).

2.1.2 Ca II The Ca II H and K transitions at λ3933.7 and λ3968.5 arise in the chromospheres of cool stars and are frequently used to identify mass motions and the presence of circumstellar material in luminous stars (Reimers 1977a). These lines appear as a deep absorption doublet, in the center of which a chromospheric emission core is found. The emission may itself be centrally reversed, which causes the appearance of two emission peaks (see Figure 3). If differential expansion (or contraction) is present in the line-forming region, these peaks may be unequal in intensity and the central line core shifted and asymmetric as the line opacity is moved to the blue (or red), respectively. Expansion causes the long-wavelength peak to be strengthened relative to the short-wavelength peak. Such an asymmetry was first detected in the He I λ10830 line from planetary nebulae (Vaughan 1968) that were believed to be expanding. Hummer & Rybicki (1968) confirmed this interpretation, and subsequent calculations extended the results to spherically symmetric and expanding atmospheres (Kunasz 1973, Noerdlinger & Rybicki 1974). Calculations for the Sun have demonstrated that other motions [for instance, acoustic pulses (Heasley 1975), "microturbulence" (Shine 1975), periodic oscillations (Gouttebroze & Leibacher 1980), and mass-conserving outflow (Dupree 1981)] can contribute to asymmetric profiles.

In the luminous stars, narrow absorption features are frequently found (see Figure 3) in the Ca II profiles. These features usually occur at shorter wavelengths than corresponding lines in the stellar photospheric spectrum and are generally attributed to a circumstellar shell; interstellar absorption lines may be present as well.

Ca III recombines to Ca II in the outer reaches of a stellar atmosphere, producing ample amounts of Ca II that result in a narrow absorption feature. The material producing this feature is generally thought to be at

or near the asymptotic flow velocity of the wind. The measured velocities of this feature show a decrease from about 80 km s^{-1} for the early K giants to 25 km s^{-1} for early M giants. Supergiant stars exhibit a similar decrease in velocity with spectral type from about 40 km s^{-1} in the G and late K supergiants (with some as high as 140 km s^{-1}) to $\sim$10 km s^{-1} by spectral type M. These values are less than the surface escape velocity. The circumstellar Ca K features can be variable on a time scale of one to several months in K giants, and minor changes can occur within days (Reimers 1977a). A few luminous stars also exhibit redshifted narrow lines perhaps associated with inflowing material (Reimers 1977a).

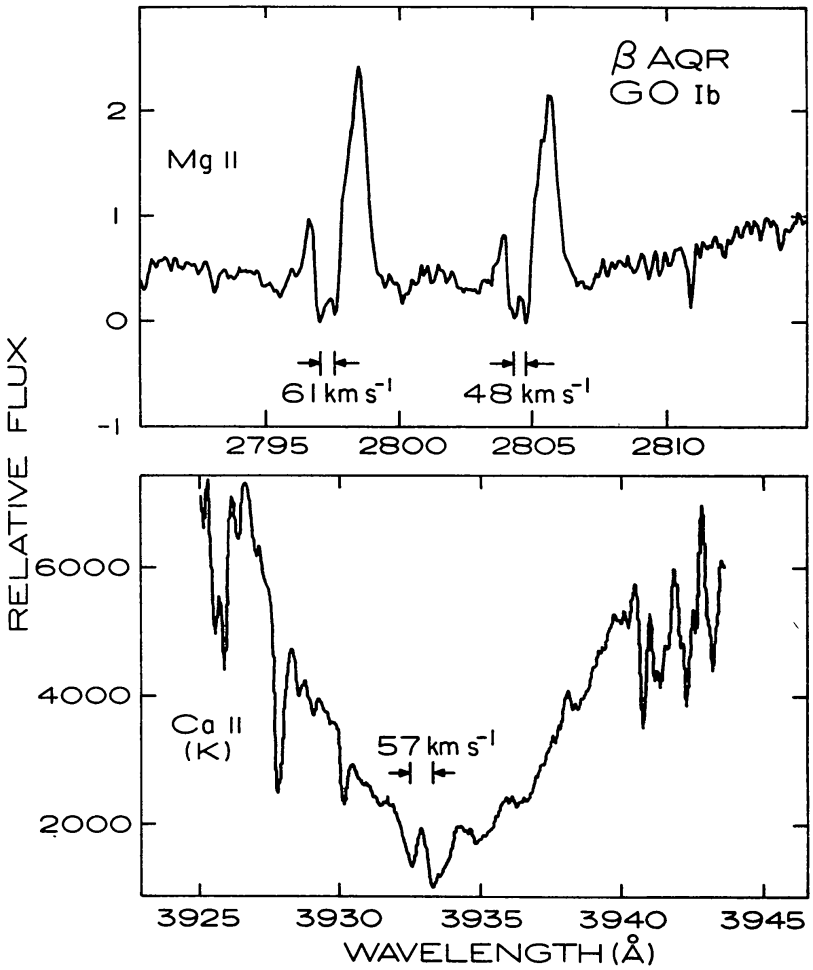

Figure 3 Ca II (K) line and Mg II profiles in the "hybrid" supergiant β Aqr. The absorption component near the rest wavelengths results from an intrinsic chromospheric line reversal approximately at line center on which interstellar absorption is superposed. The narrow high-velocity absorption (~ -60 km s^{-1}) arises in the expanding stellar atmosphere; it is frequently taken to indicate the terminal velocity of the wind (but see text), and its presence is dubbed circumstellar absorption (figure from Dupree 1981).

Dwarf stars do not show asymmetric Ca II profiles signifying outflow. The Sun, when observed in integrated light (White & Livingston 1978), shows a profile that is slightly asymmetric in the sense of a downflow, namely the violet emission peak is more intense than the red peak. The Ca II line becomes more symmetrical as solar activity increases (Oranje 1983). Surveys of the Ca II profile in other dwarf stars indicate symmetric profiles or asymmetry in the sense of downflow (see compilation by Linsky et al. 1979a). In dwarf stars, calcium does not reflect the wind structure of the outer atmosphere because it is formed in the low chromosphere (Vernazza et al. 1981), before ordered outward motion dominates, and it is ionized in the corona and the hot ($\sim 10^6$ K) solar wind.

2.1.3 He I The He I (λ10830) transition is a high excitation chromospheric line arising from a metastable level that is $\sim$20 eV above the ground term. In the Sun, the line is partially controlled by the photoionization of neutral helium by the coronal extreme ultraviolet and soft X-ray flux (Milkey et al. 1973, Avrett et al. 1976) and displays weakening over the surface when these high-temperature emissions decrease, as in coronal holes (Harvey & Sheeley 1977). This transition has been observed in a number of stars (Zirin 1976, and references therein); most recently, it was detected in 70 luminous stars by O'Brien (1980) using a Reticon detector so that spectra with good signal-to-noise ratios were obtained. The profiles are sometimes difficult to interpret, however, because of blending with adjacent photospheric Si II, Ti I, and telluric lines. The absorption line of λ10830 is weak and frequently broad. It is just noticeable in mid and late F-type supergiants and increases in strength by G0 spectral type. All K stars exhibit the λ10830 line, but it is not detectable at about spectral type M1. The line is most frequently present in absorption, but the proportion of stars with absorption profiles decreases with spectral type, since emission becomes apparent. The stars with λ10830 emission are thought to be losing mass, as is inferred from other diagnostics—principally the Ca II K asymmetry. In the G-type supergiants α Aqr and β Aqr, a P Cygni profile is found that has variable emission strength. The line center may correspond to the stellar radial velocity, but the absorption cores are variable and asymmetric with absorption extending to -200 km s^{-1}. For these supergiants, such a value is close to the escape velocity and commensurate with the values found from high-resolution spectra of the Mg II transition (see Section 2.2.1). Another G supergiant (ε Gem) shows multiple absorption components at -19 and $+30$ km s^{-1} (O'Brien 1980) that are similar to multiple components found in the Ca II λ8542 transition (Linsky et al. 1979b).

Thus, in luminous F and G stars, the λ10830 line appears to originate

in regions where the material has already undergone substantial acceleration. It seems unlikely that this occurs in a narrow region deep within the chromosphere. A similarly extended emission peak is not observed to longer wavelengths. The most attractive explanation is that the line is formed in an extended atmosphere. Varying emission also suggests that discrete mass-loss events may be occurring (O'Brien 1980). A comprehensive non-LTE study of the He λ10830 line has not been made for low-gravity conditions, and O'Brien's observations suggest that it could be a valuable wind signature.

2.1.4 CIRCUMSTELLAR LINES Circumstellar lines of low-ionization species such as Na I, Ca I and II, Al II, and Fe I provided the first spectroscopic evidence of mass loss (Deutsch 1956). Subsequently, many researchers have measured these lines to derive mass-loss rates. The circumstellar features are not observed in spectra of dwarf stars, and they appear predominantly in spectra of luminous cool giants and supergiants. The observed profiles result from an assumed symmetric photospheric absorption line upon which is superposed the typical P Cygni profile of a line formed in an extended expanding atmosphere. The velocity of the absorption core is taken to represent the expansion velocity of the shell or line-forming region. The column density of circumstellar material is estimated from the asymmetries in the line or by using curve-of-growth techniques (Hagen 1978).

There are several difficulties that can make the derived mass-loss rate uncertain [see discussion in Bernat (1982) or Hagen (1980)]. The radius at which the absorption occurs must be inferred by independent means. Additionally, the optical spectral region does not contain the dominant stages of ionization expected in a circumstellar envelope for the abundant elements; thus assumptions are required concerning the ionization equilibrium, or else the use of minor ions. Another concern arises from the confusion with truly interstellar features. Since the wind velocities of these stars tend to range from 5 to a few tens of km s^{-1}, precisely in the expected range of interstellar lines, in many cases it is a problem to separate the two (D. Reimers, personal communication, 1986).

2.2 *Ultraviolet Lines*

The ultraviolet region has several unique advantages in the study of mass loss when the spectral resolution is sufficient for profile and velocity measurement. Most strong resonance lines of abundant species occur in the ultraviolet, which allows stellar winds of all temperatures (10^4–10^6 K) to be detected through appropriate ionic species; moreover, species in the dominant stage of ionization can usually be sampled. Semiempirical

modeling and evolution of mass-loss rates are more reliable when dominant ionization stages can be used; in addition, resonance-line profiles are more sensitive in many cases to local physical conditions than are the subordinate lines, which makes them better diagnostics of atmospheric structure. However, narrow features in strong stellar resonance lines can suffer from confusion with the spectrum of the interstellar medium, and the stellar line profile can be affected to some degree (Bernat & Lambert 1976, Böhm-Vitense 1981, Drake et al. 1984). Several criteria are frequently used to discriminate between the two absorption sources, namely velocity differences between the star and the interstellar gas, variability in the stellar spectrum, or model profiles.

2.2.1 Mg II TRANSITION The Mg II resonance doublet (λ2795.5 and λ2802.7) is similar in appearance to the Ca II resonance transition with a centrally reversed emission core. In the high-gravity atmosphere of the Sun (and other dwarf stars), the magnesium transitions are formed in regions near the calcium transition (Vernazza et al. 1981, Lites & Skumanich 1982). In low-gravity atmospheres, the Mg II profile can exhibit substantial asymmetry of the emission cores (see Figure 3) due to differential expansion in the chromosphere and opacity in the expanding atmosphere. Calculations suggest that Mg II is a dominant state of ionization in the far wind or envelope due to the relatively high rate of recombination (see Dupree 1982). Thus the Mg II profile, particularly the short-wavelength portion, is especially sensitive to the structure of the outer atmosphere.

Much attention has been given to determining the appearance of the Mg II line throughout the HR diagram because it is an easily accessible strong feature in the spectrum of a cool star. In a study of 19 giant and supergiant Population I stars, Stencel & Mullan (1980a,b) found the Mg II k line to change asymmetry from short-wavelength peak $\geq$ long-wavelength peak ($S \geq L$), indicative of downflow, to $S < L$, indicative of outflow, with decreasing effective temperature of the star (see Figure 4). Stencel & Mullan (1980a,b) proposed that there is a dividing "line" marking the asymmetry changes, which, if real, would suggest a sudden onset of wind and mass loss. However, the reality of such a "line" is open to question from studies such as that of the four giant stars in the Hyades cluster (Baliunas et al. 1983). These giants have very similar physical properties, yet three of them show a violet < red ($S < L$) peak asymmetry and the other a violet > red ($S > L$) peak asymmetry. If the apparent asymmetry resulted from the interstellar medium, it should be similar for all the giants. The stellar profiles of the Hyades giants must be intrinsically different, and the position of these stars in Figure 4 at $M_v \approx +0.7$ and

$V-R = 0.73$ is not in harmony with the dividing "line." The presence of such a dividing line does not seem established, and there may well be other as yet unidentified parameters that determine the appearance of mass outflow as measured in the Mg II line.

Narrow absorption features occurring at high velocities on the violet side of the Mg II lines are formed in the expanding stellar envelope, and their velocities are identified with the asymptotic flow velocity of the wind. Typical velocities for this narrow absorption feature are 60–100 km s^{-1} for yellow supergiant and bright giant ("hybrid") stars (Hartmann et al. 1980, Reimers 1982). The cooler giants and supergiants exhibit much lower outflow velocities in optical and ultraviolet lines of neutral and singly ionized metals. Absorption features from the wind, if present, would lie within the core of the Mg II reversal, where it would be difficult to separate such absorption from that of an interstellar component.

The terminal wind velocities in the luminous "hybrid" stars may be higher than 100 km s^{-1}. Deep exposures of one star, α TrA (K4 III), reveal broad absorption troughs in the Mg II line that extend up to -180 km s^{-1} (Hartmann et al. 1985). Such values are particularly interesting because

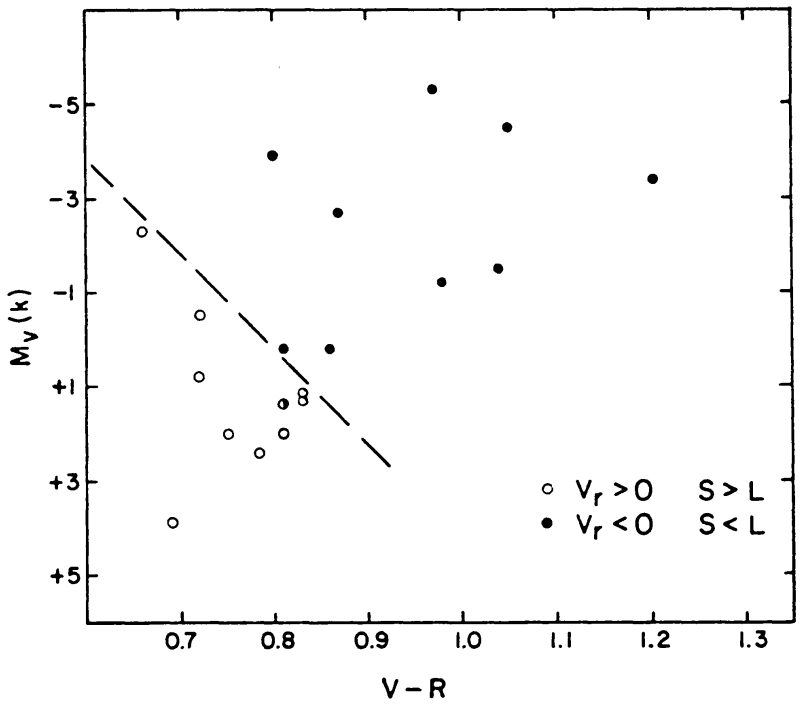

Figure 4 Observed asymmetry of the emission peaks of the Mg *h* and *k* lines. Filled circles denote stars with a negative radial velocity V_r in which the short-wavelength peak (S) is weaker than the long-wavelength peak (L). Open symbols designate the opposite: $S > L$ and $V_r > 0$ ($S/L \sim 1$ for the half-filled circle, α UMa). The broken line represents the locus along which the asymmetry reverses (figure from Stencel & Mullan 1980b).

they are comparable to the surface escape velocity (~ 150 km s^{-1}) for this star and demonstrate that the asymptotic wind velocity can be substantially higher than indicated by the narrow "high-velocity" absorption features. A recent study (Reimers & Che-Bohnenstengel 1986) of 22 Vul (G3 Ib–II) also concluded that high expansion velocities ($\approx -160 \pm 20$ km s^{-1}) are present.

The Mg II profiles exhibit variability in the few supergiant stars that have been observed frequently. The short-wavelength portion of the line profile varies in α Aqr (G2 Ia) on a time scale of about 1 yr (Dupree & Baliunas 1979); α Ori (M2 Iab) has shown variability of a factor of 2 in the Mg II emission line (Dupree et al. 1984c, 1986) that appears due to changes in circumstellar absorption and perhaps intrinsic chromospheric emission. The high-velocity circumstellar shell absorption and short-wavelength emission in γ Aql, θ Her, and α TrA (Figure 5) also show variations on a time scale similar to α Aqr (Hartmann et al. 1985). Because similar changes were not observed in the fluxes of other ultraviolet chromospheric lines (with the exception of α Aqr), these observations suggest that to first order the Mg II opacity is varying in the distant wind, and that it is wind variability rather than chromospheric variability that is detected.

There are some cases of intrinsic chromospheric variability of Mg II in giants (Mullan & Stencel 1982, Brosius et al. 1985). Binary systems of giant stars also show modulation associated with spot activity (see Section 6).

2.3 *Radio-Frequency Emission*

Continuum radio-frequency emission arises from bremsstrahlung in the ionized plasma in a stellar atmosphere. Thus, a measure of the radio flux can be related to the amount of ionized material in the source. Both Panagia & Felli (1975) and Wright & Barlow (1975) derived simple expressions for the radio flux from a star undergoing mass loss, namely

$$S_\nu = 5.12 \left[\frac{\nu}{10\ \text{GHz}}\right]^{0.6} \left[\frac{T_e}{10^4\ \text{K}}\right]^{0.1} \left[\frac{\dot{M}}{10^{-5}\ M_\odot\ \text{yr}^{-1}}\right]^{4/3} \times \left(\frac{\mu}{1.2}\right)^{-4/3} \left[\frac{V_{\text{exp}}}{10^3\ \text{km s}^{-1}}\right]^{-4/3} \bar{Z}^{2/3} \left[\frac{d}{\text{kpc}}\right]^{-2} \text{mJy}.$$

Here μ is the mean atomic weight per electron, V_{exp} is the expansion velocity, $\bar{Z}$ the average ionic charge, and d the source distance (Panagia & Felli 1975). This approximation assumes optically thick emission, complete ionization in the envelope, constant electron temperature, constant velocity flow, a spherically symmetric envelope, and an electron density distribution

varying as r^{-2}. Subsequent studies have modified this expression for finite shells and for various density relations (Olnon 1975, Spergel et al. 1983). The continuum radio flux indicates the amount of ionized material that is being lost by the star; in many of the coolest stars, this factor can be as low as 0.01% of the total mass loss (Drake & Linsky 1983b, 1984, Spergel et al. 1983).

A small number of cool stars have been detected in the radio continuum, typically at 2 or 6 cm using the high sensitivity available with the VLA (to

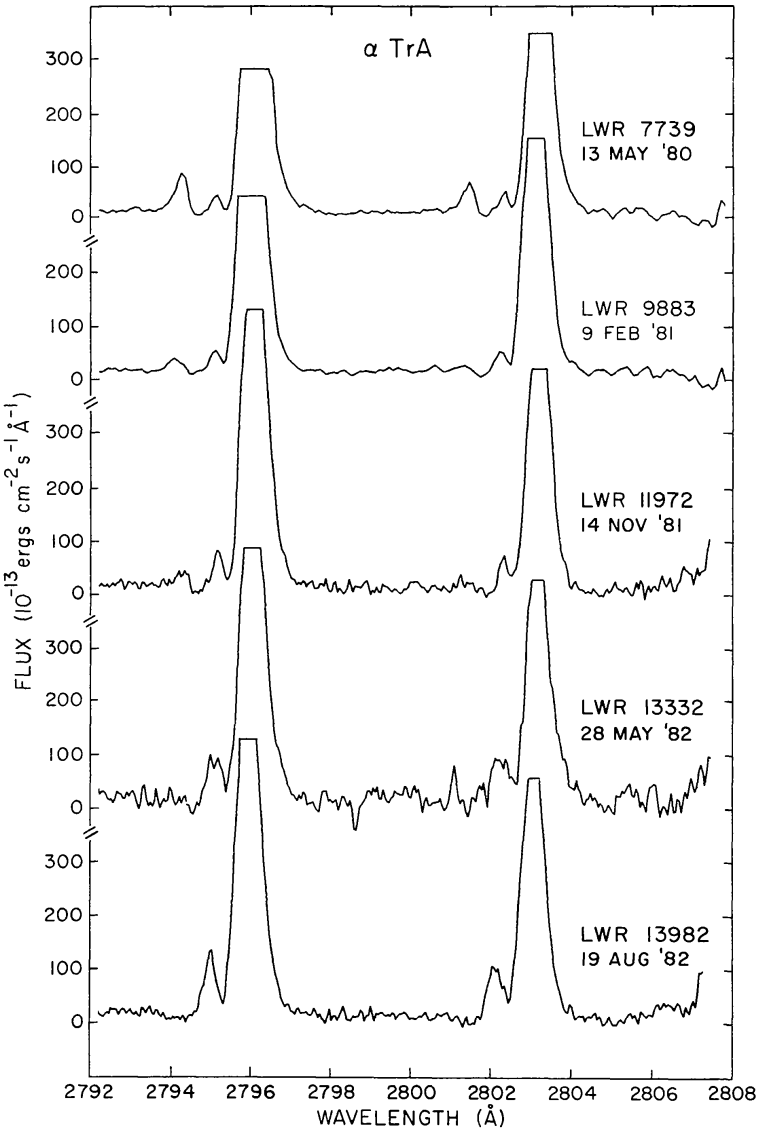

Figure 5 Mg II (*h* and *k*) line profiles in the hybrid bright giant star α TrA. The variability of the short-wavelength emission is apparent in each of these emission lines, suggesting that the wind opacity varies on a time scale of ~9 months or less (figure from Hartmann et al. 1985).

levels of $\sim$0.2 mJy). Observations of supergiant stars α Sco (M1.5 Iab+ B2.5 V) and α Ori (M2 Iab) show optically thick thermal spectra and suggest the presence of an extended warm chromosphere that is partially ionized (Newell & Hjellming 1982, Hjellming & Newell 1983). Four K and M giant stars have been detected by Drake & Linsky (1983b, 1984): β Gem (K0 III), α Boo (K2 III p), α Tau (K5 III), and α' Her (M5 II). In addition, another possible detection is β UMi (K4 III). Ionized mass-loss rates estimated from the 6-cm continuum range from 7×10^{-11} to $1.5 \times 10^{-9}\ M_\odot\ \mathrm{yr}^{-1}$. These values show no systematic trend with spectral type and are generally less than mass-loss estimates using other methods (Drake & Linsky 1984), as is expected for the coolest stars, where much of the hydrogen is neutral or in molecular form.

The VLA image of the binary system α Sco reveals two stars, separated by 2.9 arcsec, and the existence of an ionization front between the components. The nebulosity is ionized by the Lyman continuum of the B star. The Lyman continuum luminosity and the location of the ionization front enabled Hjellming & Newell (1983) to estimate the mass-loss rate from the M star as $\sim 2 \times 10^{-6}\ M_\odot\ \mathrm{yr}^{-1}$. This value exceeds by a factor of 3 the rate determined from analysis of optical circumstellar lines in high-dispersion spectra (Kudritzki & Reimers 1978); ultraviolet spectra from IUE suggest $\dot{M} \sim 1 \times 10^{-6}\ M_\odot$ (Hagen 1984).

Neutral hydrogen can be detected through the 21-cm transition. However, sensitive searches of circumstellar envelopes for this line have only yielded upper limits (Knapp & Bowers 1983). For the coolest stars, the nondetections can be understood if the hydrogen is in molecular form. For a hotter star, such as α Ori, the hydrogen is expected to be in atomic form, and the upper limit to $\dot{M}$, $\dot{M} \lesssim 5 \times 10^{-6}\ M_\odot\ \mathrm{yr}^{-1}$ (Knapp & Bowers 1983), is consistent with the multifrequency analyses discussed in Section 5.

3. THE PRESENCE OF MASS LOSS IN POPULATION I STARS

It is useful to construct a picture of mass-loss (or mass-outflow) "tracers" across the HR diagram and to compare this with the presence of other atmospheric characteristics, such as high-temperature plasma. Relationships among these quantities provide a phenomenological guide to support theoretical interpretation and allow us to draw a comprehensive picture of the mass-loss process.

One of the strongest features in ultraviolet spectra of cool stars is the C IV resonance doublet at λ1548.20 and λ1550.77. Appearance of this emission line signals the presence of plasma at temperatures $\sim 10^5$ K under the

collisionally dominated conditions expected in such an atmosphere. The presence of this transition and others is shown in Figure 6 for a variety of stars. The detection of a given spectral feature is, of course, a function of the exposure time. Stars included in Figure 6 with no C IV detection have generally had exposures sufficient to set upper limits on the order of 0.1 of the solar surface flux. Many of the detections have surface fluxes ranging from 1 to 100 times the solar value.

C IV is detected in main-sequence stars and in the hottest giant stars (through spectral type ~K2). This ion appears in conjunction with strong emission features of lower excitation species (Fe II, O I, S I, and Si II) in many luminous giants and supergiants—the "hybrid" stars—that also give evidence for a substantial wind (see Figure 7). The coolest and most luminous stars of all (roughly the late K and M giants and supergiants) show no signs of high-temperature plasma in their spectra, but mass loss is occurring, as inferred from circumstellar features and asymmetric profiles of Mg II. It is clear that a simple two-dimensional classification of temperature and gravity is insufficient to predict the character of a cool stellar atmosphere and the onset of massive stellar winds. It is also clear

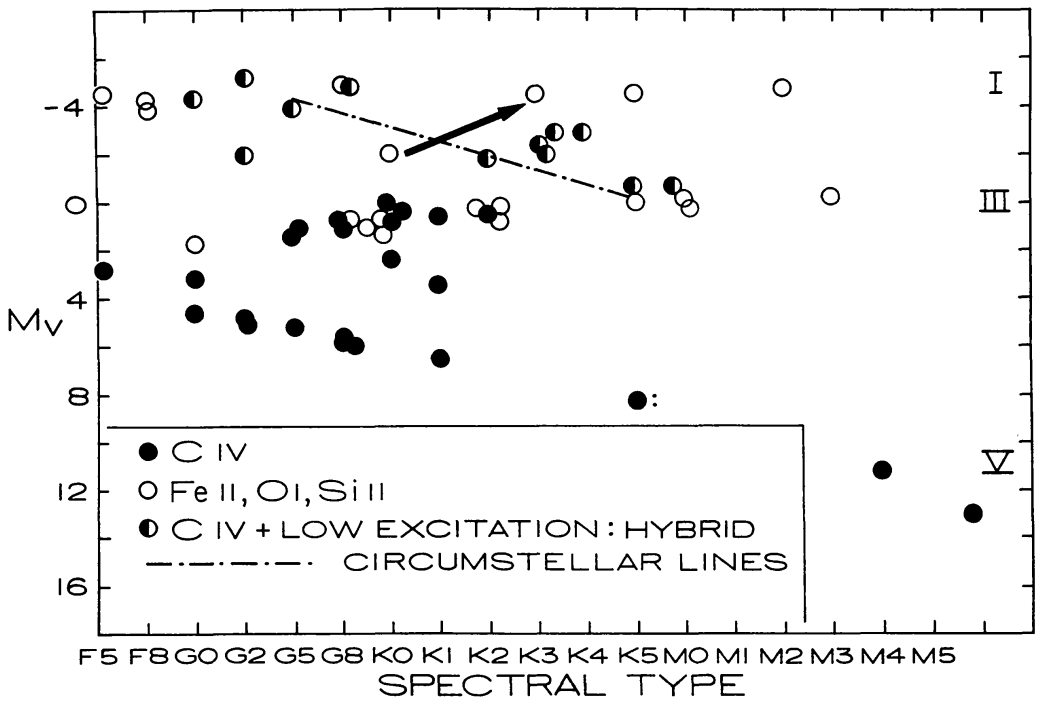

Figure 6 The presence of various spectral features in stars of different spectral types and luminosities. Stars exhibiting low- and high- (C IV) excitation species are termed "hybrid" and are denoted by the half-filled circles (Hartmann et al. 1980, 1981, 1985, Reimers 1982, 1984, 1986). The broken line denotes the boundary above which circumstellar Ca II lines appear in optical spectra (Reimers 1977a).

that abrupt "boundary lines" separating atmospheric characteristics, as were proposed at first (Linsky & Haisch 1979, Simon et al. 1982), may have a superficial appeal but are contradicted by subsequent observations. The appearance of circumstellar Ca II absorption features suggests that the stars with significant mass loss cannot maintain a high-temperature atmosphere. However, the hybrid stars are a counterexample, which, in one view, provides the connecting link between those stars showing C IV emission (and negligible mass loss) and the coolest luminous stars (Hartmann et al. 1980, 1981). These hybrid stars may represent an intermediate stage with an extended atmosphere at a temperature between the 10^6 K of dwarf stars and 10^4 K of luminous cool stars. A study of one such star, 22 Vul, suggests a wind temperature of at least $\approx$30,000 K (Reimers & Che-Bohnenstengel 1986). Alternatively, hot C IV-emitting

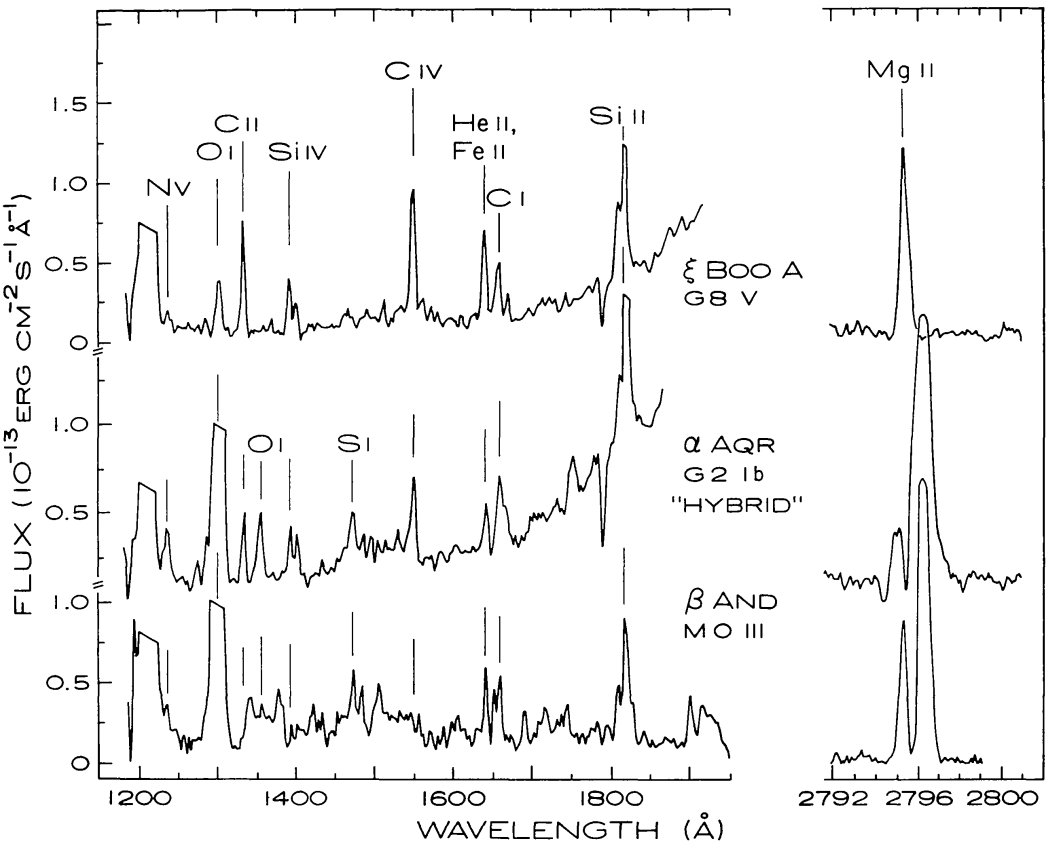

Figure 7 Ultraviolet spectra of cool stars from IUE, showing three types of cool stellar atmospheres and the detectability of winds: ξ Boo A is an active dwarf star; α Aqr (a hybrid star) possesses C IV, lower ionization species such as O I, S I, and C I, and an asymmetric Mg II line typical of an expanding atmosphere; β And exhibits only species of low excitation and a massive wind indicated by the Mg II transition. The O I (λ1300) and geocoronal Lα (λ1216) peaks have been truncated where indicated by a flat top. The data are from Hartmann et al. (1982).

plasma may be confined within magnetic loop structures holding fast in the presence of a massive cool wind.

X-ray emission has a distribution among stars in the HR diagram that is similar to that of the C IV transition (Figure 8), with X rays generally detected from main-sequence stars and a smattering of giants, many of which are active binary systems or rapidly rotating stars (Vaiana et al. 1981, Helfand & Caillault 1982). Although C IV emission represents one characteristic of the hybrid stars, these stars do not show X rays in the 0.3–4 keV energy range to a level ~ 0.3 of the quiet soft X-ray emission in the Sun (Ayres et al. 1981), whereas the C IV surface flux is typically a few times the quiet Sun value (Hartmann et al. 1982). There has been some discussion about whether X rays are in fact produced in the atmosphere but then absorbed by the massive stellar wind (Ayres et al. 1981, Hartmann et al. 1981). Comparing the observed relative emission measures for N V and X rays for various stars with theoretical predictions for conductively dominated coronal loop structures, Hartmann et al. (1982) find a generally lower X-ray emission measure for hybrids than for dwarf stars for an

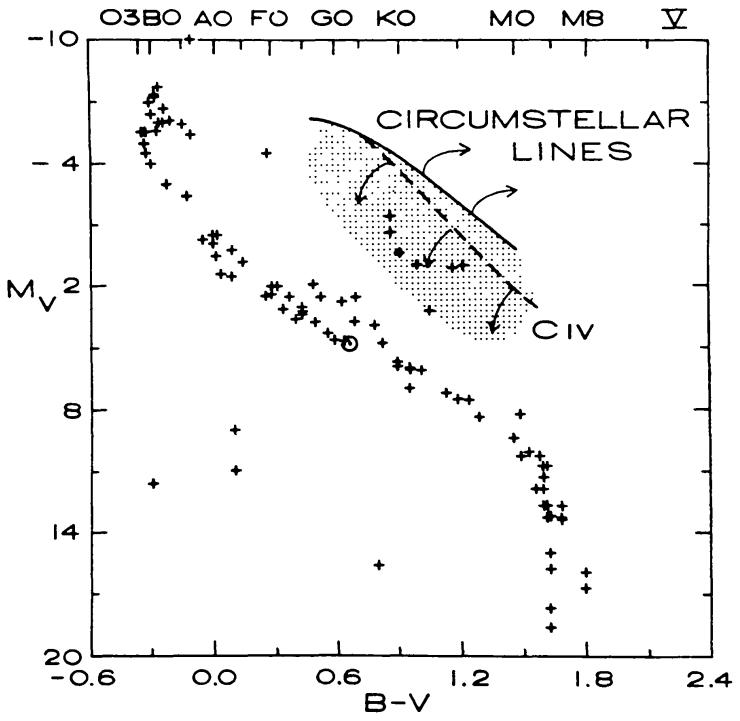

Figure 8 Relation between soft X-ray emission and optical and ultraviolet spectral features. Stars that have been detected by the stellar survey on HEAO-2 ("Einstein"), as described by Vaiana et al. (1981), are denoted by +. The position of the Sun is indicated by an open circle. The hatched region corresponds to the locus of hybrid stars, and is also the location where stars may display high- or low-temperature emission lines. The C IV "boundary" is indicated by a broken line. The appearance of stars with circumstellar Ca II absorption (Reimers 1977a) is indicated (figure from Dupree 1981).

equivalent N V strength, although the amount of X-ray-emitting material may be consistent with other low-gravity stars. Observations have generally set only upper limits for the hybrid stars, and it would not be surprising to find X rays at some level that are undetectable at present. One nearby hybrid star, α TrA, has recently been detected by Brown (1986) using EXOSAT.

Many of the spectral features indicating mass loss are shown in the composite HR diagram in Figure 9. Among the hottest stars, the first widely detectable indication of mass loss is the asymmetry of the Mg II line due to this ion's high opacity in a recombining wind, followed by the asymmetry in Ca II in cooler and more luminous stars as the expansion becomes substantial in the low chromosphere. In contrast to the Sun, where there is a close resemblance between the behavior and appearance of the Ca II and Mg II transitions (Lites & Skumanich 1982), these profiles in stars of lower gravity and temperature are frequently quite disparate (refer, for instance, to Figure 3). Such behavior can be sorted out with detailed semiempirical modeling, but the extended nature of the atmosphere clearly must be a major cause. O I is another spectral feature that signals an extended atmosphere due to fluorescence with Lβ; Figure 7 shows its strength in the luminous stars. Application of the C II density diagnostic at λ2300 supports the great extent ($\approx 2\ R_*$) of the chromosphere in the coolest luminous stars (Carpenter 1984, Carpenter et al. 1985).

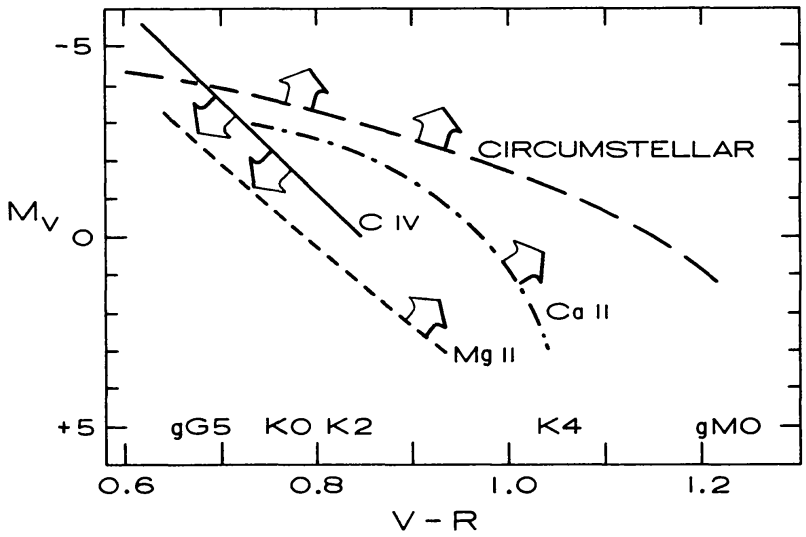

Figure 9 The appearance of various spectral features as a function of color and luminosity. C IV emission is prominent to the left of the solid line (but see Figure 6); the asymmetry of the emission peaks in Mg II and Ca II indicates outflow to the right of the appropriate broken lines (Stencel 1978, Stencel & Mullan 1980a,b). Circumstellar Ca II absorption features are found above the long broken line (Reimers 1977a).

The Lα profile is potentially a very sensitive probe of outflow, but it has been measured in only a few bright stars. Lα profiles obtained by the *Copernicus* satellite suggested that outflow motions were detectable in stars on the giant branch, before asymmetries in Mg II and Ca II (Dupree 1976) were noted.

4. MASS LOSS FROM DWARF STARS

4.1 *The Sun*

The Sun is the only cool single dwarf from which mass loss has been observed to date, and that by in situ measurement of the solar wind in the interplanetary medium, for the most part in or near the ecliptic. The mass loss from the Sun as measured in the equatorial wind corresponds to $2 \times 10^{-14}\ M_\odot\ \mathrm{yr}^{-1}$ and does not appear to vary over the solar cycle by more than a factor of 2 (see Zirker 1981). Coronal mass ejections, the sudden expulsion of material, may account for 5 or at most 10% of the steady-state mass loss (Wagner 1984, Howard et al. 1985). When the Sun is viewed as a star, in integrated light without spatial resolution, there is no spectroscopic evidence for mass loss. It is only with spatially resolved images and spectroscopy that surface activity can be delineated and the Doppler shifts and line asymmetries arising from motions can be detected. The Sun provides an example of the relationship between winds, mass loss, and surface activity that most probably exists at some level on other stars.

X-ray and ultraviolet images of the outer solar atmosphere, taken most frequently during the *Skylab* era of 1973, revealed a very inhomogeneous atmospheric structure. To a first approximation, it could be described by its magnetic field characteristics. Regions of increased magnetic field on the solar surface, "active regions," were evident in the corona in the looping structures indicative of closed magnetic field lines and in the enhanced radiative losses in these structures. Regions of weak and diverging magnetic fields, coronal holes, had reduced line emission and were identified as the source of high-speed solar wind streams (Krieger et al. 1973, Withbroe & Noyes 1977). The source of low-speed flows appears to be coronal streamers and sector boundaries (Gosling et al. 1981, Neugebauer 1983). Open magnetic field structures in the corona allow material to escape easily (Bohlin 1977, Zirker 1977). Although the mass flux can be comparable in each of three types of flow (from coronal holes, boundaries, and transient events), the major fraction of the total solar mass loss arises from coronal holes (Neugebauer 1983). During solar maximum, major coronal holes are not present, and yet the solar wind continues. At that time, there undoubtedly is mass loss from other open-field regions all over the Sun that are not as spatially extended as the coronal holes.

4.2 *Spectroscopic Detection of Solar Mass Loss*

Experiments subsequent to those on *Skylab* were able to measure fluid motions and line profiles in restricted regions of the solar atmosphere in an attempt to detect the onset of the solar wind. Sunspot umbrae show upflows in the chromosphere-corona transition region amounting to a mean value of 1.2 ± 5.6 km s^{-1} (Kneer et al. 1981, Gurman & Athay 1983). However, the large-scale flow measured in the C IV line near active regions is consistent with widespread loop structure exhibiting downflow (Athay et al. 1983, Dere et al. 1984). The variations of the dominant flow pattern in the transition region are illustrated by the observations of Brueckner et al. (1977), who simultaneously measured the hydrogen Lα profile and the Doppler shift of the C IV transition at different points on the Sun. There is a great deal of scatter between the degree of asymmetry of the Lα profile and the apparent C IV velocity. However, the general trend is clear—outflow at higher levels where C IV is formed occurs in conjunction with a long-wavelength > short-wavelength line asymmetry in Lα and vice versa. This measurement simply indicates that atmospheric motions of plasma at temperatures between 10^4 and 10^5 K are continuous, and it affirms a stellar spectroscopic diagnostic. Calculations of line profiles of Mg II and Ca II under mass-conserving outflows in a quiet Sun model display a similar long-wavelength > short-wavelength asymmetry (Dupree 1981). Correlation of such asymmetries with direct measurements of outflow or downflow by Brueckner et al. (1977) gives reassurance to the interpretation of similar asymmetric line profiles in stars.

A coronal hole has a marked signature on the solar disk in the high-transition region lines ($T \gtrsim 7 \times 10^5$ K). It appears weaker as compared with the neighboring quiet Sun regions (Huber et al. 1974). Lines formed at lower temperatures can be slightly fainter in coronal holes than in the quiet Sun; some low chromospheric lines formed indirectly by coronal EUV continua may also show weakening below coronal holes. Outflow associated with coronal holes appears at temperatures of about 3×10^5 K, as is evidenced in the O V line (λ629) with a measured velocity of -7 km s^{-1} and Mg X (λ625) exhibiting an outflow velocity of -12 km s^{-1} (Rottman et al. 1982, Rottman & Orrall 1983, Orrall et al. 1983). Earlier measurements in a presumed open-field region that was associated with a coronal hole (Cushman & Rense 1976, 1977; see Rottman et al. 1982) showed outward velocities of -16 km s^{-1} at coronal levels (Si XI, Mg IX, Mg X). A magnetically quiet region on the disk revealed Doppler shifts of the Fe XII (λ1349.4) line amounting to 17 km s^{-1} in the radial direction (Brueckner et al. 1977). Dere (1983) has cautioned that velocity measures

on the disk are usually relative to lower chromospheric features, and the amount of true outflow may be uncertain.

Spectroscopic measurements of the acceleration region of the solar wind (2–4 $R_\odot$) using coronagraphic techniques suggest flow velocities at 4 $R_\odot$ of -100 km s^{-1} (Withbroe et al. 1982, Kohl et al. 1983), a value corresponding to -14 km s^{-1} at 1.5 $R_\odot$ that is in harmony with the spectroscopic measures on the disk. None of these values is close to the escape velocity from the solar surface of 610 km s^{-1}, or 305 km s^{-1} at 4 $R_\odot$. Outward motion has also been discovered in the fast-moving (400 km s^{-1}) jets of material observed in transition-region lines C IV and Si IV and others (Brueckner & Bartoe 1983). The mass and energy flux injected into the corona by these abrupt events is estimated to be comparable to that lost by the solar wind. Dere (1983) and Brueckner & Bartoe (1983) have suggested that if these events prove to be quite common, then they may be the source of the wind and lead to very inhomogeneous structures close to the Sun.

4.3 *Structure of the Solar Wind*

The varied sources and characteristics of the wind emerging from the rotating Sun lead to complex structures in the outer heliosphere. Recent exhaustive reviews of observations and theoretical models have been given by Burlaga (1984), Hundhausen (1985), and Pizzo (1985). High-speed streams from a restricted region such as a coronal hole can overtake slower moving material in the wind and coalesce to form a corotating stream, as first noted by Parker (1963). These streams are characterized at large heliocentric distances ($\sim$5 AU) by abrupt jumps in velocity, which are interpreted as shock fronts with increased density, temperature, and pressure behind the velocity increase (Gosling et al. 1976). At greater distances from the Sun ($\sim$10 AU) as the stream evolves, the original high velocities have decayed, and corotating pressure waves develop. Nonlinear interactions among pressure waves are expected to occur at still greater distances ($\sim$25 AU) from the Sun (Burlaga 1983). About 100 days is required for a feature in the solar wind to reach 25 AU. Such a time encompasses about three solar revolutions, during which the solar source region can change and transient activity such as mass ejections (Wagner 1984) will occur. One might expect a complex three-dimensional configuration of stream interactions to be present between transient and corotating streams.

Corotating streams have been proposed by Mullan (1984a,b) to explain Mg II and Ca II absorption features and to provide a source of high-temperature ($\sim 10^5$ K) emission in cool luminous stars. But a recent estimate (Brosius & Mullan 1986) of the high-temperature emission for a

hybrid star suggests that these corotating interaction regions will not contribute to the observed N V flux unless substantial density enhancements are present. The conditions for existence and the character of these structures have yet to be evaluated quantitatively for stars other than the Sun. Coalesced shocks in low-gravity stars do not lead to dense extended atmospheres, and hence the mass-loss rates are predicted to be rather low (Wood 1979, Holzer & MacGregor 1985). In the hybrid luminous stars, narrow absorption features in Mg II and Ca II vary in intensity on a time scale of months (Reimers 1977a, Hartmann et al. 1985). In one such star, α Aqr (G2 Iab), the Mg II wind opacity increased concurrently with an increase in high-temperature emissions (C IV), an observation that signals inhomogeneities in the atmosphere as well as in the wind (Dupree & Baliunas 1979). Periodic variations in such emissions have been sought (Brosius et al. 1985), but more observations are required to be confident of the presence of rotational modulation in luminous stars.

4.4 *Composition of the Solar Atmosphere and Wind*

Abundance determinations from different levels and features within the solar atmosphere can be made, since wavelength coverage with high-resolution spectroscopic techniques coupled with spatial resolution of individual features is now possible. Additionally, many measurements of energetic particles in the solar wind have been obtained under varied conditions of solar activity. These observations suggest that the compositions of the solar corona, associated energetic particles, and the solar wind are similar to each other but differ from that of the photosphere (Cook et al. 1980, Mewaldt 1980, Veck & Parkinson 1981). Meyer's (1985a,b) recent compilations demonstrate that heavy-element abundances in the corona, the solar wind, solar energetic particles, and galactic cosmic rays are depleted by factors of 4 to 6 (for cosmic rays) from their solar photospheric values for elements with first ionization potentials $\gtrsim 9$ eV.

The depletion mechanism is not completely understood but believed to result from a basic physical process in the solar atmosphere, perhaps a preferential acceleration mechanism that enables ions (with first ionization potential <9 eV) to move into the corona from the photosphere more efficiently than neutral species (Veck & Parkinson 1981, Cook et al. 1980, Geiss 1982). Geiss & Bochsler (1984) have suggested that the ionization-dependent depletion may involve hydrogen Lα photoionization and the preferential acceleration of ionized species in spicules. A process is required that operates under the turbulent conditions of a chromosphere with constant spicule activity, although a magnetic field may help to constrain plasma motions. Mariska (1980) found from extreme ultraviolet spectra that the C,N,O abundances relative to Si are the same in the quiet Sun,

a coronal hole, an active region, and a prominence. This result suggests a common transport mechanism is involved irrespective of atmospheric structure or magnetic configuration. In addition, high-precision measurements of the composition of flare-accelerated material using *Voyager* 1 and 2 (Breneman & Stone 1985) demonstrate that flare-to-flare abundance variability depends on the charge-to-mass ratio (Q/M) of the ion. Such a result is not unexpected, since a particle's rigidity [$\approx 1/(Q/M)$] controls acceleration and propagation processes.

A coronal abundance that is altered from photospheric values will affect the inferred structure of a stellar atmosphere and introduce another uncertainty in determining the energy balance of a stellar atmosphere. The extent to which preferential transport occurs in a low-gravity, low-temperature atmosphere is not known. But some theoretical models show the potential impact of varying abundances. Holzer et al. (1983) note that the structure of a stellar wind (i.e. temperature, density, flow speed, wave energy flux) depends upon the composition because it influences radiative losses and damping rates in the case of Alfvén wave–driven winds.

4.5 *Other Implications for Stellar Observations*

Extrapolating these observations to other cool dwarf stars suggests that high-temperature ("coronal") lines must be detected in order to measure outflows. This will require spectroscopic instruments operating at least in the 900–1200 Å range, and preferably at shorter wavelengths. In addition, the star may only display outward plasma motion when a large area of the disk is covered by open magnetic field structures. Such a configuration might occur only at stellar activity cycle minimum. Since total emission can be dominated by contributions from the denser active regions, a particularly propitious distribution of activity over a stellar disk may be required. It may be necessary to find a star that is oriented pole-on to us. Whereas a line sensitive to coronal radiation (e.g. He I λ10830; see Zirin 1976) might signal weakened coronal regions and perhaps coronal holes, only coronal plasmas give evidence for sustained outward motions. Weaker transitions of coronal species that occur above λ912 (e.g. Fe XII λ1349) must be used in addition to the transition region lines of N V, O V, and O VI. Strong transitions from high-ionization stages lie from 150–300 Å and should be accessible. Coronal holes on the Sun are not all alike, and lines other than the "solar" diagnostics may be useful in the coolest dwarf stars. Separating a true outflow leading to mass loss from a circulation pattern, as evidenced in the complex loop structures in the solar chromosphere and transition region, will require high-resolution spectroscopy.

High-velocity (~ -250 km s^{-1}) emission features have been observed

(Weiler et al. 1978) in the Mg II transition in two short-period RS CVn binary systems: HR 1099 (G5–K0 IV+G5 V) and UX Arietis (G5 V+K0 IV). Such events may be associated with transient radio events detected simultaneously, rather than with a continuous mass-loss process. But at present we do not know the frequency of such high-velocity events.

5. MASS-LOSS RATES FROM EVOLVED LUMINOUS SINGLE STARS

Only a few stars have available spectra of sufficiently high quality and broad frequency coverage to encourage serious attempts at a derivation of the mass-loss rate. The previous discussions in this review note the disadvantages and difficulties with a single diagnostic of mass loss. There is no analysis to date that has satisfied all of the observational material for a star to better than a factor of five. In many cases, the deficiencies of the models lead to more subtle inferences concerning the atmospheric structure than is possible from a less detailed approach. Continual refinement of observations, theoretical methods, and fundamental atomic physics may well change the results discussed below.

5.1 *Alpha Bootes*

One of the first attempts to interpret chromospheric line profiles by defining atmospheric structure and deriving a mass-loss rate was made by Chiu et al. (1977) using Ca II and Mg II profiles of Arcturus (α Boo; K2 IIp). A model chromosphere based principally on the Ca II H and K lines (Ayres & Linsky 1975) was used in a plane-parallel geometry with an arbitrary mass-conserving outflow, chosen to fit as best as possible the Mg II (k) and Ca II (K) line profiles. Two-level model atoms and complete frequency redistribution in the line cores were assumed. Chiu et al. find a mass-loss rate of $8 \times 10^{-9}\ M_\odot\ \mathrm{yr}^{-1}$ from their calculations. Subsequent interpretation of the blueshifted Mg II (K) absorption feature (Ayres et al. 1982) led to lower values, $>3 \times 10^{-10}\ M_\odot\ \mathrm{yr}^{-1}$ up to $2 \times 10^{-9}\ M_\odot\ \mathrm{yr}^{-1}$ if a wind of higher density is present. A further calculation with a spherical geometry and assumption of partial frequency redistribution for the Mg II line (Drake & Linsky 1984) reduced the value of $\dot{M}$ still further to $\sim 1 \times 10^{-10}\ M_\odot\ \mathrm{yr}^{-1}$. The ionized component of the wind as measured in the 6-cm continuum flux with the VLA (Drake & Linsky 1983b, 1984) gives a lower value, as expected, of $\sim 7.5 \times 10^{-11}\ M_\odot\ \mathrm{yr}^{-1}$. Through these early stages of calculations, the inferred mass-loss rate has changed by a factor of 80, thus illustrating the difficulties with simple approximations to the complex problem of line transfer and the constraints of a few observations.

5.2 *Alpha Orionis*

Physically consistent models have been constructed for the supergiant α Orionis (Betelgeuse; M1–2 Ia–Iab) by Hartmann & Avrett (1984) in an attempt to understand the energetics of the extended atmosphere and secondarily to obtain a mass-loss rate. They adopted the theory of Hartmann & MacGregor (1980) by requiring damped Alfvén waves to produce an atmosphere extending several stellar radii with low terminal expansion velocity. The calculations were carried out in spherical geometry, partial frequency redistribution was assumed as necessary to calculate the hydrogen ionization balance, and the temperature structure was varied until the calculated radiative losses were in harmony with the heating rate obtained from wave dissipation. This model was then used to predict many line profiles and a number of observed quantities relating to the presence of an extended atmosphere: the continuum radio flux as a function of frequency, cores of Hα and the Ca II infrared triplet, fluxes and profiles of chromospheric lines, and speckle imaging of the circumstellar environment in Hα. Whereas the observed free-free radio emission and the extended Hα atmosphere are well matched by the model, the observed line profiles and fluxes show substantial deviations from the predictions. These difficulties lead to the suggestion that the supergiant atmosphere may be in a "quasi-static" condition, with complex internal motions in the low chromosphere. Downflows may be prevalent, such as those indicated by the asymmetric Fe II emission lines (Boesgaard 1979). The mass-loss rate associated with this model is $1.4 \times 10^{-6}\, M_\odot\ \mathrm{yr}^{-1}$, a value that is consistent with most other determinations (see Table 1).

Complex velocity and brightness changes of the photosphere have long

Table 1 Recent determinations of $\dot{M}$ for α Orionis

$\dot{M}$ ($M_\odot\ \mathrm{yr}^{-1}$)	Technique	Reference
$\lesssim 5 \times 10^{-6}$	H I	Knapp & Bowers 1983[a]
4×10^{-6}	Surface brightness in K I	Mauron et al. 1984
3×10^{-6}	Si II circumstellar	Hagen et al. 1983
1.4×10^{-6}	Semiempirical models (optical and ultraviolet)	Hartmann & Avrett 1984
1.2×10^{-6}	CO ($J = 1$-0)	Knapp & Morris 1985
$>4 \times 10^{-7}$ to $\lesssim 2 \times 10^{-6}$	CO ($J = 2$-1)	Knapp et al. 1980
$<1.4 \times 10^{-8}$	400 μm (dust)	Sopka et al. 1985

[a] Using the VLA, Bowers & Knapp (*Ap. J.*, in prep.) have just detected 21-cm H I emission from α Ori that suggests $\dot{M} = 2.2 \times 10^{-6}\, M_\odot\ \mathrm{yr}^{-1}$.

been attributed to α Orionis (Guinan 1984, and references therein). In addition, the configuration of the star may be even more complicated by the identification of two close cool stellar companions (Karovska et al. 1986). Line profiles of Mg II changed subsequent to the periastron approach of one companion; such profile changes could result from varying acceleration in the supergiant atmosphere, perhaps caused by the companion, or from fluctuations in the intrinsic chromospheric emissions (Dupree et al. 1986). The surface brightness of the 10-μm continuum flux from one side of the extended atmosphere has decreased over one year—a change that has been ascribed to agglomeration of dust grains that are partially opaque (Bloemhof et al. 1985). Simple models of emission from the circumstellar envelope do not provide a good fit to the tentatively observed line profile of the 2.6-mm CO transition (Knapp & Morris 1985), and a mass-loss rate of $1.2 \times 10^{-6}\ M_\odot\ \mathrm{yr}^{-1}$ was derived. Clearly, α Ori is a many-faceted system, and the presence of varying mass loss cannot be excluded.

5.3 *Envelopes of Luminous Stars*

Expanding circumstellar envelopes in the coolest stars produce a P Cygni feature in the line of Sr II at λ4077. Because this ion is the dominant stage of ionization in a circumstellar envelope, it eliminates uncertain corrections for ionization equilibrium and is attractive for deriving the gas column density. Using the Kunasz-Hummer code, Hagen (1978) modeled the Sr II profile to consist of a photospheric absorption line modified by the contribution of an extended scattering envelope. With the assumption of a shell expansion velocity ($10\ \mathrm{km\ s}^{-1}$), the gas column densities are derived.

Dust grains surrounding M giants and supergiants radiate in the infrared. An emission feature at 10 μm originates from silicate grains and can be used to estimate the column density of dust. With a radial distribution of dust inferred from photometry at 20–33 μm, as well as a model of the dust composition (Hagen 1982), optical depths can be obtained. Mass-loss rates follow given the additional assumptions of solar abundances, a stellar radius for giants ($500\ R_\odot$) and supergiants ($1000\ R_\odot$), and an inner shell radius ($10\ R_*$). The combined dust and gas mass-loss rates derived by Hagen et al. (1983) in this way vary from $<8 \times 10^{-8}\ M_\odot\ \mathrm{yr}^{-1}$ for the early giants to 2×10^{-8}–$2 \times 10^{-6}\ M_\odot\ \mathrm{yr}^{-1}$ for the supergiant stars.

Emission from CO occurring in circumstellar envelopes of evolved stars is sensitive to mass-loss rates $\gtrsim 3 \times 10^{-8}\ M_\odot\ \mathrm{yr}^{-1}$. Knapp and colleagues have surveyed more than 100 cool evolved stars and have detected about half of these in the CO transition, $J = 1$-0 (Knapp & Morris 1985), and many in the $J = 2$-1 line (Knapp et al. 1982). These objects comprise Mira variables, C and S stars, and a few supergiants. Observed line profiles are matched to models of optically thin or thick circumstellar shells.

Terminal velocities of the flows range from 8 to 25 km s^{-1}; mass-loss rates have values from $\approx 3 \times 10^{-8} M_\odot$ yr^{-1} (the lower limit of detectability) to $2 \times 10^{-4} M_\odot$ yr^{-1}.

Results for giant and supergiant stars are shown in Figures 12 and 13 and are discussed in the context of parameterization of mass loss in Section 8.

6. MASS LOSS FROM STARS IN BINARY SYSTEMS

6.1 *Zeta Aurigae/VV Cephei Systems*

Spectroscopic eclipsing binary stars consisting of a red giant (or supergiant) and a hot companion can be used to advantage in evaluating the mass loss from red giant components. Since the scale of the system is known, one of the major uncertainties is eliminated from determination of the mass-loss rate (see discussions in Sanner 1976, Bernat 1977, Hagen 1978). However, the analysis is still complex for many reasons. The two stars and the circumstellar shell are generally not resolved, so that observed lines arise from the whole scattering expanding envelope. Instead of simple absorption lines, P Cygni profiles are measured. To analyze such profiles requires consideration of radiative transfer in three dimensions with nonspherical geometries. The presence of the companion brings additional subtleties to the analysis, as discussed by Che et al. (1983). The hot companion may affect the wind structure and mass loss as a result of the modification of the local gravity in the vicinity of the primary star, the time-dependent ionization and recombination conditions, and the effects of shocks that result from the hot star's supersonic motion through an expanding envelope. Hempe (1982), and Che et al. (1983) have developed methods to analyze line profiles in binary systems of the ς Aur/VV Cep type. These systems consist of a cool supergiant (spectral type K–M) with an extended atmosphere and a hot B star companion; orbital periods are on the order of 1000 to several thousand days, indicating that the separation of the two stars is ~ 5 K star radii. The K supergiant envelope is believed to extend as much as 1000 K star radii (Hempe 1982). P Cygni lines are formed by scattering of the B star photons within the expanding envelope of the K star. An atlas of profiles for these systems has been calculated with a two-level approximation using escape probability methods (Hempe 1984). These profiles should aid subsequent analyses.

Ultraviolet spectroscopy provides a wealth of resonance and some high-excitation lines: C II, IV; N I; O I; Mg II; Al II, III; Si II, III, IV; S II; and Fe II, III. To date, analysis has focused on low-excitation lines of C II, Mg II, Si II, and Fe II. The mass-loss rates from the K supergiants in three binary systems (Che et al. 1983) (Figure 13) range from 0.6–4 $\times 10^{-8} M_\odot$ yr^{-1}.

Observations at various phases are particularly useful. The variation of absorption-line depth is sensitive to the turbulent velocity in the wind when the B star is in front of the supergiant, and to the terminal velocity of the flow when the B star is behind the supergiant (Che et al. 1983). Observations at different phases in three systems suggest $V_\infty \sim 40$–80 km s^{-1} and $V_{\text{turbulent}} \sim 20$–$30$ km s^{-1}. If continuous outflow and a value for $\dot{M}$ is assumed, then line profiles at different phases can be used to derive a velocity and density profile in the atmosphere (Schröder 1985). This is necessary to understand the requirements for driving mechanisms of the wind.

6.2 *RS CVn Stars*

These binary systems consist of a hot component of spectral type F to G and of luminosity class IV or V, show orbital periods between 1 and 15 days (although systems with longer periods exist), and display strong Ca II H and K in emission. X-ray observations, ultraviolet and optical spectroscopy, and photometry show these stars to have enhanced chromospheric and coronal emissions and extreme forms of stellar activity (Walter & Bowyer 1981). In some systems, asymmetric profiles of chromospheric resonance lines have been found that indicate mass outflow. Capella (α Aur; G0 III+G5 III) is one such system that displays strong Lα asymmetry (Dupree 1975, Ayres 1984), although lines of ions such as Si IV and C IV do not indicate any measurable outflow with value greater than the IUE resolution ($\sim$20 km s^{-1}) (Ayres 1984).

A particularly interesting example of possible mass loss associated with surface inhomogeneities is found in λ And (G7–G8 IV–III+?), which has displayed a symmetric profile of Ca II K and Mg II k during a phase of low photometric brightness (associated with star spots) and an asymmetric profile (indicative of outflow) during its bright phase (when spots are absent) (Baliunas & Dupree 1982). Such behavior suggests an inhomogeneous atmospheric structure with mass flow present at specific stellar phases. This morphology is also consistent with a simple solar analogy of atmospheric regions containing open and closed magnetic structures.

The evolutionary status of many of these systems suggests that the components have evolved as single stars tempered by mild mass exchange and probably mass loss (Popper & Ulrich 1977), although there is little direct evidence for mass loss in RS CVn systems. Multiple emission-line components of Mg II have been found with velocities up to -250 km s^{-1} in HR 1099 (Weiler 1978), and λ And has shown transient emission features in Ca II K at moderate expansion velocities (Baliunas & Dupree 1979). High-mass-loss rates ($>10^{-8}\ M_\odot$ yr^{-1}) have been suggested (Hall 1972, 1976) for RS CVn systems, but values of this order would drive the stars

out of synchronism, and soft X-rays, observed to be strong, would be absorbed by the copious atmospheric material implied by these high rates (De Campli & Baliunas 1979). Moderate mass loss, 10^{-9}–10^{-11} $M_\odot$ yr^{-1}, would be in harmony with the X-ray measures (Weiler et al. 1978).

6.3 *Symbiotic Stars*

Symbiotic stars consist of a late-type giant or bright giant and a fainter companion—a main-sequence star or a hot star. The continuum spectrum of systems with a main-sequence component is best explained by the presence of accretion from the red giant, with $\dot{M} \sim 10^{-5}\, M_\odot$ yr^{-1} (Kenyon & Webbink 1984, Kenyon 1986, and references therein). Such a high rate and the continuum colors suggest that Roche lobe overflow provides the source of mass. However, the systems with hot stellar components appear to require accretion in order to maintain high temperatures (Paczynski & Rudak 1980, Tutukov & Yungelson 1982). This accretion requires $\sim 10^{-9}$–$10^{-7}\, M_\odot$ yr^{-1}, implying that the red giant loses $\sim 10^{-7}$–$10^{-5}\, M_\odot$ yr^{-1}. The higher values represent systems containing a Mira variable (Kenyon 1986).

7. MASS LOSS FROM METAL-DEFICIENT STARS

7.1 *Theoretical Motivation*

The problem of reproducing the color-magnitude diagram of globular cluster stars by numerical calculations first directed attention to mass loss in the red giant phase. Over a decade ago, it was realized that an *assumption* of mass loss in globular cluster giant stars could explain the observed color distribution of horizontal branch stars (Iben & Rood 1970, Castellani & Renzini 1968). Models of stellar evolution indicate that the blue horizontal branch stars are lower in mass by $\sim 0.2\, M_\odot$ than the stars at the main-sequence turnoff (Rood 1973, Renzini 1981). The assumption of significant steady mass loss from the asymptotic giant branch (AGB) stars reduced the calculated maximum luminosity of the AGB tip and brought theoretical models into better agreement with the observed color-luminosity diagram of galactic globular clusters (see Iben & Renzini 1983). Calibration of the relative ages of globular clusters in other galaxies by using the extent of the AGB above the tip of the first giant branch requires a similar understanding of the mass-loss rates in AGB stars (Mould & Aaronson 1982). A change in the mass-loss rate by a given factor causes the same change in the derived age (Iben & Renzini 1983).

While it may be that invocation of mass loss to explain discrepancies between theory and observation simply represents one convenient and well-known "*refugium peccatorum*" (Castellani et al. 1985), other processes

have emerged that may be important. Convection core overshoot and semiconvection have been included in models of stellar interiors (Maeder & Mermilliod 1981). The process of overshoot from hydrogen- or helium-burning convection zones has the effect of increasing the size of the degenerate CO core, decreasing the mass at which stars undergo an asymptotic giant branch (AGB) phase (the so-called M_{up}), and hence decreasing the luminosity of stars in the AGB phase (Castellani et al. 1985, Renzini et al. 1985). Thus, the need for high-mass-loss rates to explain the dearth of luminous AGB stars may be lessened or perhaps even eliminated entirely. Stellar rotation has been suggested as an influence on the mass loss of stars, modifying the color distribution of luminous massive supergiants (Pylyser et al. 1985, Sreenivasan & Wilson 1985) and increasing the proportion of blue horizontal branch stars in globular clusters by extending a star's lifetime on the giant branch, where mass loss occurs (Fusi-Pecci & Renzini 1978). Measurements of the rotation of horizontal branch stars by Peterson (1983, 1985) are consistent with the latter suggestion. This review focuses on mass loss, but these other ideas certainly merit continued investigation.

Lacking empirical estimates of the mass-loss rates in luminous stars, theorists most frequently have used a relation of the type

$$\dot{M}(M_\odot\,\mathrm{yr}^{-1}) = -4 \times 10^{-13}\eta L/gR,$$

where all quantities are in solar units, and η is an empirical fitting factor. This relation, with $\eta = 1$, was constructed by Reimers (1975b) based on a dimensional analysis for 16 Population I red giant stars. Surprisingly, with a scaling factor η ranging from 0.25 to 1 (Aaronson & Mould 1982, Mould & Aaronson 1982, Renzini 1981, Iben & Renzini 1983), the morphology of the HR diagram is reasonably well matched in both galactic and Large and Small Magellanic Cloud (LMC and SMC) globular clusters. The variation of AGB tip luminosity with cluster age for globular clusters in the SMC and LMC led Aaronson & Mould (1985) to suggest that higher mass-loss rates than the Reimers (1975b) relation are required for the most luminous stars ($M_{bol} < -5$) corresponding to clusters with ages less than $\sim$2 Gyr. Higher mass-loss rates would contribute to the observed absence of luminous AGB stars in the LMC and terminate their evolution to higher luminosities (Reid & Mould 1984). Lifetimes on the AGB are typically 10^6 yr, and mass-loss rates of 10^{-6}–10^{-7} $M_\odot$ yr^{-1} yield the desired mass loss of 0.2 $M_\odot$.

In addition to steady mass loss, a phase of substantially increased mass loss may occur. Paczynski & Ziolkowski (1968a,b) were the first to suspect that a relationship existed between long-period variables and planetary nebulae. Evolution on the AGB may proceed with a quiescent wind until

the star begins pulsating in the fundamental mode at a luminosity dependent upon the stellar mass. This pulsation degenerates into relaxation oscillations, during which mass loss or envelope ejection takes place in rapid fashion (Sparks & Kutter 1972, Wood & Cahn 1977, Tuchman et al. 1979). Calculations of pulsation processes have been reviewed by Wood (1981). This phase of ~ 10 yr, during which as much as $10^{-3}\ M_\odot\ \mathrm{yr}^{-1}$ is lost, has been dubbed a "superwind" by Renzini (1981), but there is only indirect evidence for its occurrence. That photometric variability occurs in the brightest red giants in globular clusters is well documented (for instance, Walker 1955, Frogel et al. 1981, Welty 1985), but its relationship to pulsation and to enhanced mass loss has not yet been demonstrated. Willson & Bowen (1984) have suggested that pulsation will substantially enhance mass loss, such that the most evolutionarily significant mass loss will occur as a result of pulsation in post-main-sequence stars.

7.2 *Direct Evidence for Mass Loss*

The apparent faintness of metal-deficient stars makes difficult the search for signatures of mass loss that must be carried out at high dispersion. Cohen (1976) detected emission in the wings of the Hα lines in four globular cluster red giants. This emission was ascribed to an optically thin shell or circumstellar envelope, and mass-loss rates of $\sim 10^{-8}$–$10^{-9}\ M_\odot\ \mathrm{yr}^{-1}$ have been derived (Cohen 1976, Mallia & Pagel 1978, Cacciari & Freeman 1983, Gratton 1983). Subsequent measures of the Hα emission phenomenon demonstrated that emission above the continuum is detectable in about 61% of stars when $\log L_*/L_\odot > 2.7$, and emission is not apparent below this luminosity cutoff (Gratton et al. 1984). A systematic dependence of the emission on metallicity is not evident, although there does appear to be a dearth of Hα emission stars in clusters with red horizontal branches. Clusters such as 47 Tuc, NGC 6717, and M71 show such deficiencies (Gratton et al. 1984).

Most relevant to the interpretation of these profiles is the variability of the emission wings. Emission and its asymmetry can vary on a time scale of a few days to months (Ramsey 1979, Cacciari & Freeman 1983, Dupree et al. 1984a, Gratton et al. 1984). Inspection (Dupree et al. 1984b) of the profiles published by Cohen (1976) and Cacciari & Freeman (1983) reveals that the emission wings exhibit the characteristic signature of downflow (i.e. short-wavelength peak > long-wavelength peak) as often as that of outflow (short-wavelength peak < long-wavelength peak). The variability and asymmetries suggest that the emission wings arise in a stellar chromosphere (Reimers 1981), a conjecture confirmed by detailed semi-empirical model calculations (Dupree 1984a). In a static atmosphere, emission wings can result naturally within a warm chromosphere. The emission

wings are sensitive to the temperature structure; the asymmetry and core shift reflect the flow in the atmosphere. The calculations in Figure 10 show shallow shoulders on the line profile (model 2) as compared with the abrupt dropoff in the observed profile of HD 165195. This comparison suggests that emission may be frequently present, although it does not exceed the continuum level. Mass-loss rates derived from several Hα profiles of metal-deficient field giants suggest that $\dot{M} < 2 \times 10^{-9}\ M_{\odot}\ \mathrm{yr}^{-1}$, a factor of 20 to 50 less than the relation proposed by Reimers for Population I stars. Such values for the Hα transition, if confirmed by further studies of Ca II and Mg II transitions, are too low to significantly affect the evolution of stars on the red giant branch of globular clusters.

The signature of mass outflow to be sought is the asymmetry and blueshift of the absorption cores of optically thick lines. Determination of the presence of mass-loss signatures in a variety of stellar populations could give clues to the driving mechanisms of stellar winds. Information on line profiles of the metal-deficient stars has been confined principally to the Hα transition. Peterson (1981) presents measurements of the core shifts of Hα and the Na D line for seven red giants (including one carbon star) in galactic globular clusters, and she detects an average shift of -11.2 ± 1 km s^{-1} in the Na D line and -5.9 ± 1.1 in the Hα line. Mallia & Pagel (1978) measured Hα core shifts ranging from 0 to -13 km s^{-1} in 13 globular cluster giants, with the majority at ~ -5 km s^{-1}. Metal-deficient field giants exhibit shifts ranging from 0 to ~ -8 km s^{-1} (Smith & Dupree 1986). These measurements and others are included in Figure 11 for comparison to the presence of Ca II circumstellar lines in Population I stars. Only the coolest and most luminous of the Population II red giants display a core shift and/or core asymmetry in Hα. The presence of circumstellar Ca II absorption in Population I stars is indicated. These circumstellar lines are ubiquitous in the coolest Pop I stars, making them a "better" diagnostic than Hα, although their association with the presence of Hα asymmetries and core shifts is not one to one. In part, this may reflect the formation of the Hα core deep in the atmosphere, as noted by Zarro & Rodgers (1983) for Pop I stars. Boesgaard & Hagen (1979) find among the M giant stars that all (except for the M0 III stars) show circumstellar Ca II absorption, but only 50% show Hα asymmetries and shifts. Mallik (1982) finds blueshifts of the core of Hα on all the late G and K supergiants studied. These statistics on the Hα asymmetry do not contradict the results in Figure 11, which show a mix of asymmetries in stars more luminous than the Ca II boundary. To the extent of available high-resolution spectroscopic material, the Hα asymmetry fraction in Pop II stars is similar to that of Pop I stars (Peterson 1982).

Very few profiles have been published of the more sensitive mass-loss

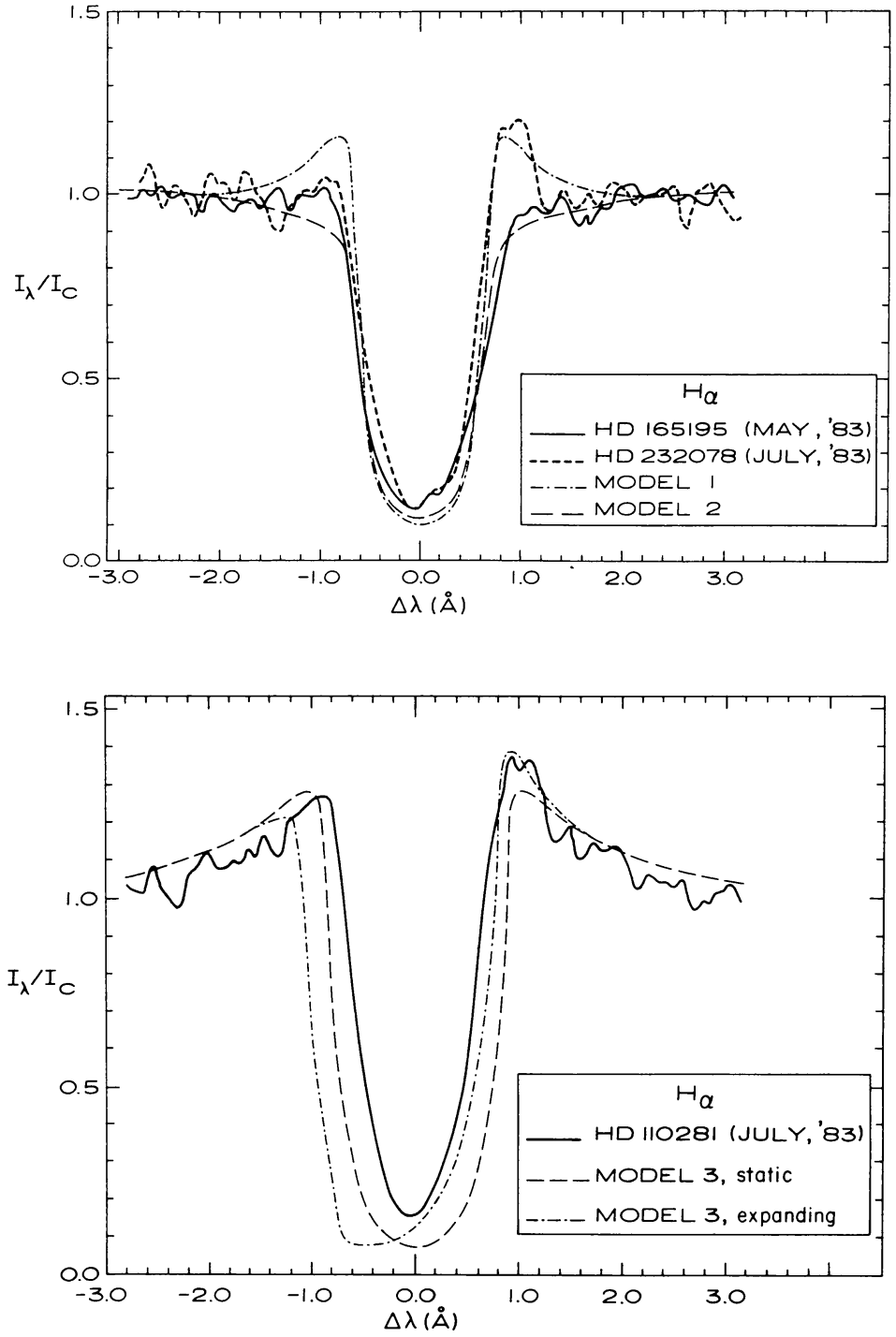

Figure 10 Calculated Hα profiles for equilibrium and extended atmosphere models (both static and expanding) as compared with the observed profiles for three metal-deficient field giants (figure from Dupree et al. 1984a).

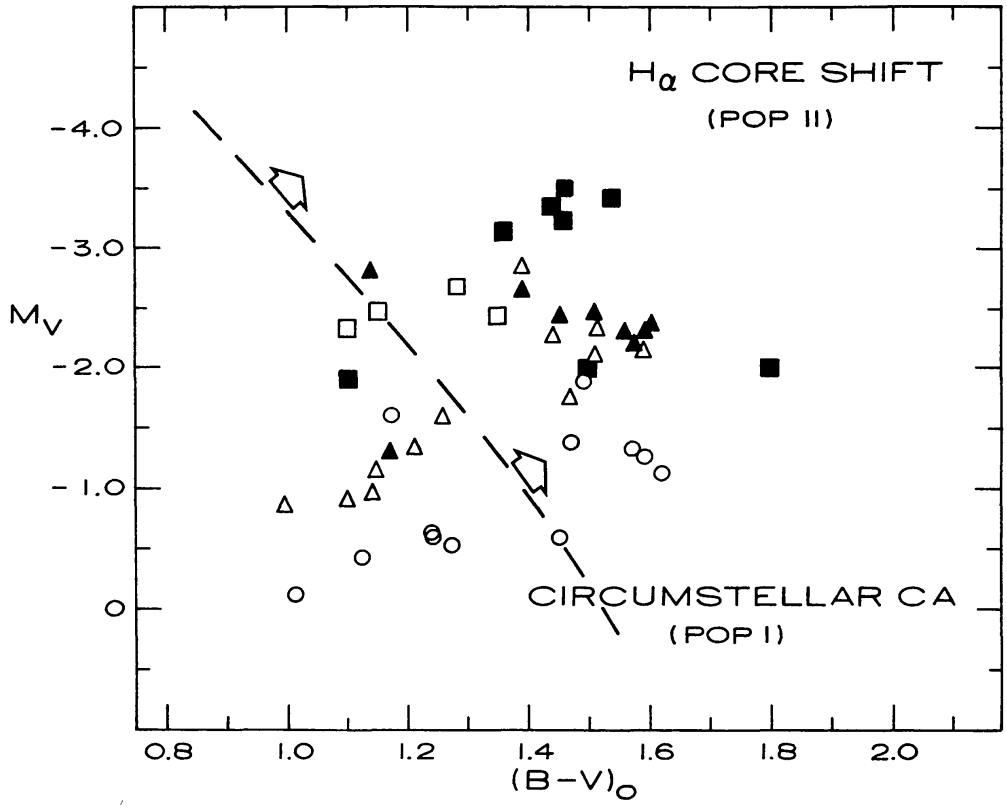

Figure 11 The presence of core asymmetries and core blueshift (filled symbols) in the Hα profiles of globular cluster giant stars and metal-deficient field stars. Open symbols denote no asymmetry or an absence of a detectable blueshift. Different shapes indicate the value of the [Fe/H] ratio as follows: ○, ● −0.25 to −0.75; △, ▲ −1.26 to −1.75; □, ■ −1.76 to −2.25. High-resolution profiles of these stars were reported in Cohen (1976), Mallia & Pagel (1978), Peterson (1981, 1982), and Dupree et al. (1984b). The broken line represents the onset of circumstellar Ca II absorption in Population I stars (Reimers 1977a) using the color calibration of spectral type versus $B-V$ from Flower (1977).

lines (Ca II, Mg II, Lα for metal-deficient stars). The Ca II profile in HD 84903, a field giant, shows evidence for an "outflow" asymmetry and a −6 km s^{-1} shift in the Hβ lines (Spite et al. 1981). The Mg II line has been detected in emission in several field giants (Dupree et al. 1984b), which indicates that chromospheres are certainly present with surface fluxes similar to Population I luminous stars, but substantial numbers of high-resolution Mg II profiles must await the Hubble Space Telescope.

8. PARAMETERIZATION OF MASS-LOSS RATES

It would be useful if the mass-loss rate for cool stars could be expressed in terms of fundamental physical quantities. Such a parameterization could give insight into the mass-loss process itself as well as provide a convenient

means of incorporating mass loss into stellar evolution calculations. The formulation proposed by Reimers (1975b), $\dot{M}$ ($M_\odot$ yr^{-1}) $\sim L/gR$ (Section 7.1), indicates that the same fraction of the stellar luminosity provides the potential energy per unit mass for escaping material. It is perhaps fortuitous that the data available at that time provided such a straightforward relationship. Goldberg (1979) used similar measures of $\dot{M}$ and demonstrated that equally good "fits" were obtained with other parameterizations, namely $\sim MR^{1/2}$ (following Mullan 1978) or $\sim R^2$, with the latter relation suggesting simply that the mass loss is proportional to the area of the stellar surface.

For a variety of luminous stars, values of $\dot{M}$ from spectroscopic as well as continuum techniques are assembled in Figures 12 and 13. Both the

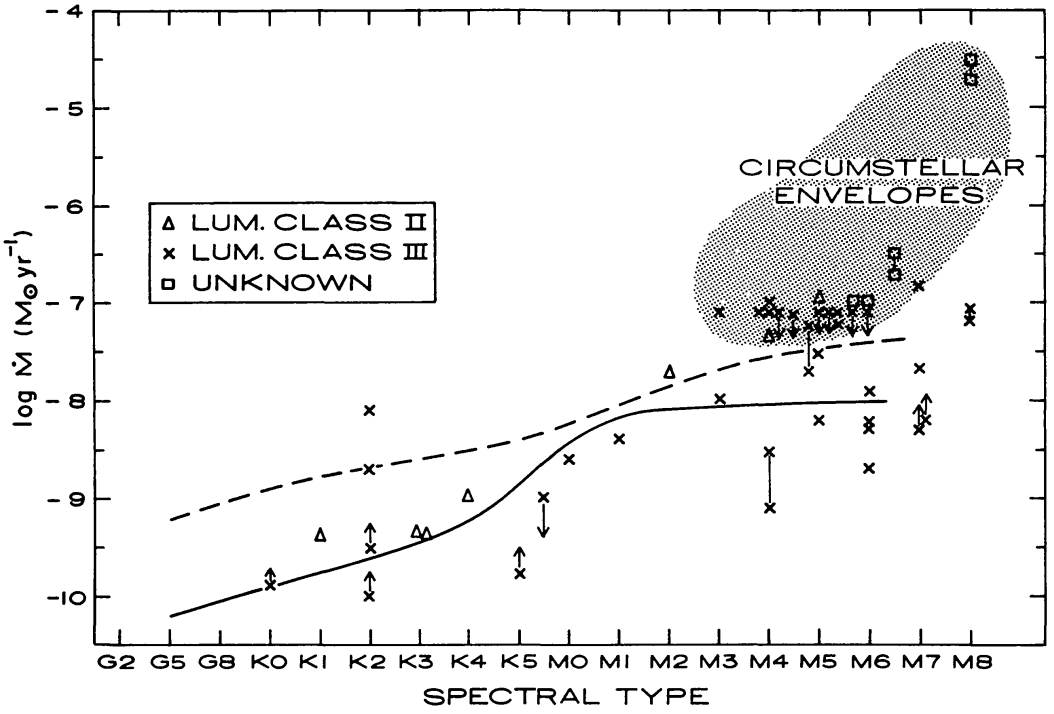

Figure 12 Mass-loss rates determined for giant stars by optical or ultraviolet lines or 6-cm continuum measurements (lower limits). The locus of rates for circumstellar envelopes (dotted area) is derived from observations of the infrared excess (Gehrz & Woolf 1971), OH sources (Bowers et al. 1983, de Jong 1983), CO (2-1) line (Knapp et al. 1982), and the CO (1-0) transition (Knapp & Morris 1985). The solid line represents $\dot{M} = -4 \times 10^{-13}\ L/gR$ from Reimers (1975b); the broken line is proportional to R^2. Values of L, g, and R for giant stars are taken from Allen (1973) except for spectral type M, where typical gravities are from Luck & Lambert (1982) and radii were computed from the data in Ridgway et al. (1980) and Hoffleit (1982). Mass-loss rates for individual stars were taken from Ayres et al. (1982), Boesgaard & Hagen (1979), Brosius & Mullan (1986), Drake & Linsky (1983a,b, 1984), Dupree et al. (1984a), Hagen et al. (1983), Reimers (1977b, 1978), Reimers & Schröder (1983), and Sanner (1976). These rates were derived using optical circumstellar lines, ultraviolet chromospheric circumstellar features, or the 6-cm radio continuum.

Reimers (1975b) relation as well as a straightforward $\sim R^2$ relation are shown in these figures. Neither one is obviously preferable, and there is still considerable scatter from a simple relation.

Giant stars have increased mass-loss rates with later spectral type, and the rates are generally lower by a factor of 10 than those for supergiant stars. There is easily a factor of ± 10 in the derived mass-loss rate at any given spectral type. Supergiant stars show an equally large scatter in $\dot{M}$ without a systematic dependence on spectral type. In fact, the analysis of Hα profiles of K supergiants by Mallik (1982) yields rather similar values (10^{-5}–10^{-6} $M_\odot$ yr^{-1}) of $\dot{M}$ from late G to early M supergiants. Semi-empirical models (Brosius & Mullan 1986) of hybrid supergiants using ultraviolet lines suggest 1–2 $\times$ 10^{-9} $M_\odot$ yr^{-1} for α Aqr (G2 Ib) and β Aqr (G0 Ib). Supergiants of earlier spectral type can have substantially lower

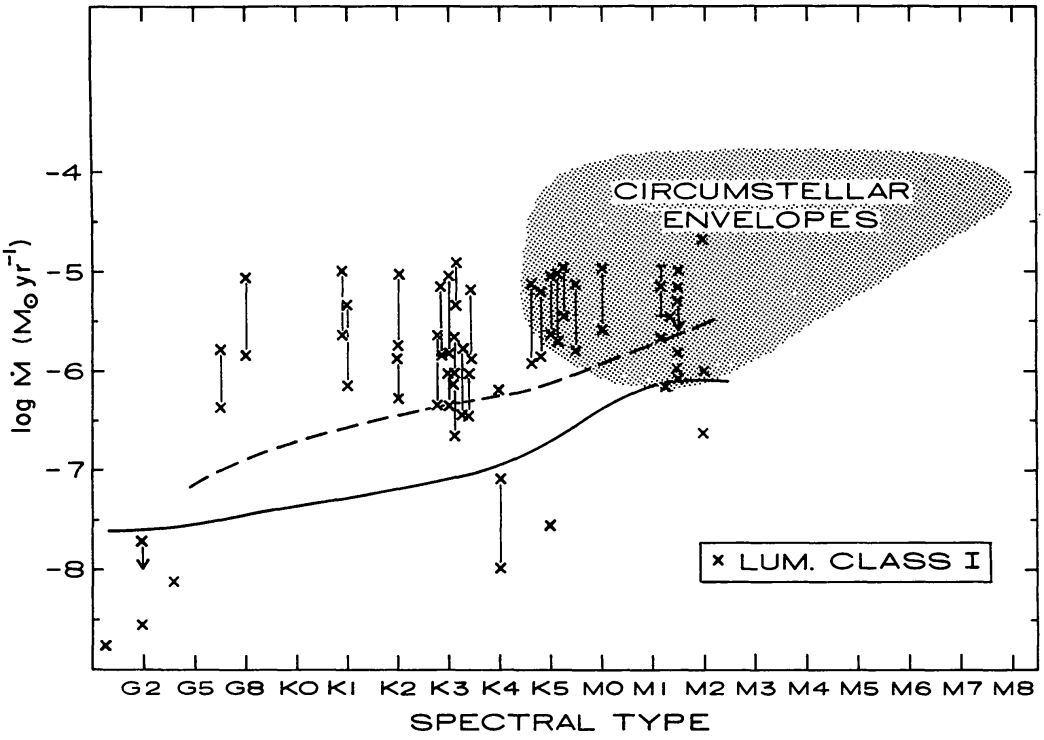

Figure 13 Mass-loss rates determined for supergiant stars. Data points for individual stars are taken from Bernat (1982), Brosius & Mullan (1986), Brown et al. (1984), Che et al. (1983), Che & Reimers (1983), Hagen et al. (1983), Kudritzki & Reimers (1978), Mallik (1982), Mauron et al. (1986), Reimers & Che-Bohnenstengel (1986), Sanner (1976), and van der Hucht et al. (1980). The cluster of points near M1–M2 represents measures of α Orionis that span a factor of 12.5 from various techniques: CO and/or K I circumstellar absorption (Jura & Morris, 1981, Knapp et al. 1982, Mauron et al. 1984), 21-cm H I (Knapp & Bowers 1983), circumstellar lines (Reimers 1975a,b, Hagen et al. 1983), and multifrequency modeling (Hartmann & Avrett 1984). Rates from circumstellar envelopes were taken from Gehrz & Woolf (1971) and de Jong (1983). As in Figure 12, the solid line represents $\dot{M} = -4 \times 10^{-13}\, L/gR$ (Reimers 1975b), and the broken line indicates $\dot{M} \sim R^2$.

mass-loss rates. Detailed profile analysis of HR 1040 (A0 Ia) and α Cyg (A2 Ia) indicates $\dot{M} \sim 8 \times 10^{-8}$ and 1.7 to $4 \times 10^{-7}\ M_\odot\ \mathrm{yr}^{-1}$, respectively (Kunasz et al. 1983, Kunasz & Morrison 1982). Higher rates are inferred from circumstellar CO 2.3-μm lines detected in ρ Cas (F8 Ia) and HR 8752 (G0 Ia), namely $>7 \times 10^{-4}$ and $8 \times 10^{-5}\ M_\odot\ \mathrm{yr}^{-1}$ (Lambert et al. 1981). Both stars are photometrically variable, and such a high mass-loss rate may be either a transient phenomenon or a reflection of a complex atmospheric circulation pattern not associated with actual escape of material from the star.

Extended circumstellar envelopes with mass loss inferred from infrared continuum measures, molecular transitions, or direct imaging in molecular lines exhibit the highest loss rates of all, 10^{-4}–$10^{-7}\ M_\odot\ \mathrm{yr}^{-1}$ (see Zuckerman 1980, Goldberg 1985, and references given in the legends to Figures 12 and 13). These high rates may reflect a completely different mass-loss process—perhaps the "superwind" phenomenon driven by pulsation and aided by radiation pressure on dust particles that has been conjectured by many authors (Renzini 1981, de Jong 1983, Willson & Bowen 1984, Jura 1986).

At present, however, it does not appear possible to prefer one empirical mass-loss relation over another; moreover, any relation will still suffer from substantial uncertainties in the absolute value of $\dot{M}$ at any given position in the HR diagram. Perhaps this simply reflects the inadequacy of any two-dimensional classification of stellar activity.

9. OBSERVATIONAL CONSTRAINTS ON A THEORY OF MASS LOSS

The mechanisms of mass loss in cool stars must satisfy many observational facts (see Figure 14):

1. The mass-loss rate increases with decreasing stellar effective temperature and increasing stellar luminosity. Values of mass-loss rates for specific stars are uncertain in most cases to a factor of 5 or even 10.

2. The asymptotic velocity of the wind flow decreases with decreasing stellar effective temperature and increasing stellar luminosity. In most stars, the asymptotic velocity is observed to be less than the surface escape velocity and varies roughly as V_{esc}^2 (Reimers 1977a).

3. When acceleration is observed, it can begin at chromospheric temperatures (10^4 K) in luminous stars (luminosity classes I, II, III) as indicated by Ca II and Mg II profiles, although wind acceleration is measurable in dwarf stars (i.e. the Sun) only in ions formed at temperatures of 10^5K (N V, O VI transitions).

4. Electron temperatures of 10^6 K are present in the solar corona, which allows a thermally driven wind to exist; electron temperatures no higher than 10^4 K are spectroscopically identified in the coolest supergiants, which suggests that mechanisms other than thermally driven winds must be invoked. Atmospheres of hybrid stars contain 10^5 K material, but the temperature existing throughout the extended atmosphere and wind is not well determined. Analysis of multiplets and semiempirical modeling suggests temperatures of 3–10 $\times$ 10^4 K (Hartmann et al. 1985, Brosius & Mullan 1986, Reimers & Che-Bohnenstengel 1986).

5. The opacity in winds of luminous stars can vary on a time scale of $\sim$1 yr. The variation of the wind may be associated with surface activity, as is found (in greatly enhanced form) from some observations of RS CVn binary stars.

6. The total energy necessary to heat the solar corona and drive the wind does not vary with position on the solar surface, but the division into different loss components does appear to change depending on the atmospheric magnetic field configurations. In the Sun, the total coronal energy losses (conductive flux, radiative flux, and wind kinetic and potential energy) are comparable in quiet regions and in coronal holes (Withbroe & Noyes 1977). However, in quiet solar regions, the radiative and conductive losses dominate the wind losses; the situation is reversed in coronal

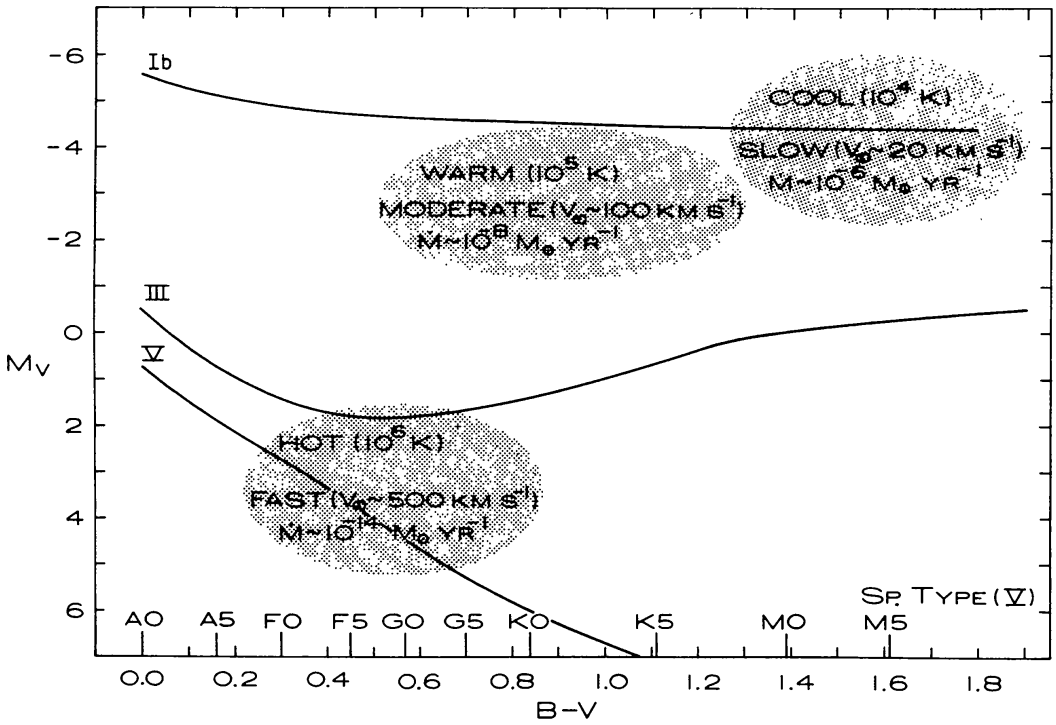

Figure 14 Characteristics of mass-loss rates and winds in stars of various luminosities (figure from Dupree 1981).

holes, where wind losses dominate. Luminous stars may be similar in energy balance to coronal holes because the energy required to lift the atmosphere out of the stellar gravitational field exceeds the radiative losses of high temperature (10^4–10^5 K) "coronal" material.

10. CONTINUING PROBLEMS

A number of problems still remain in the study of mass loss from cool stars.

1. Derivation of the actual rates for the total mass loss from a star is a complex exercise requiring a number of spectroscopic and continuum diagnostics. Only a handful of stars have well-established mass-loss rates; incomplete or simplified interpretations demonstrate that differences amounting to factors of at least 10 in $\dot{M}$ occur. The base of well-studied stars needs to be expanded before it will be possible to construct reliable mass-loss "laws."
2. Spectroscopy has been confined principally to relatively bright stars in the local neighborhood. The stellar sample of cool stars consists of objects with similar (high) metallicities. The stellar targets need to be extended to other populations. The presence and extent of mass loss under different stellar conditions and environments can give clues to the nature of the mass-loss process itself.
3. The driving mechanisms for stellar winds are not well established. Quite probably, there are several operative mechanisms, depending on the gravity, density, temperature, or magnetic field (or even other parameters) of the star. From an observational point of view, the role of pulsation and its relation to mass loss needs to be explored.
4. The extent of wind inhomogeneities and mass-loss variability can be found from continuous or long-term observations. A smattering of evidence suggests that variation may be substantial in luminous stars. It will be important to distinguish between magnetic activity cycles (perhaps influenced by large supergranulation patterns) and wind variability.
5. Atmospheric structure and the origin of line emission need to be understood, particularly in the luminous stars. Wind temperatures, for instance, are not well determined in the hybrid stars. The presence of flows and circulation patterns in the supergiants needs to be differentiated from the actual onset of continuous outward flow leading to mass loss.
6. The role of winds and their effect on the angular momentum loss of giant stars as well as dwarf and pre-main-sequence objects represents an area in which observations and analysis need to progress.

To detect mass loss, it is important to observe the appropriate signatures and to measure the significant parameters—the fluxes, the velocity shifts, the line profiles—to enable a true quantitative comparison with theoretical models. To be sure, such measurements are not easy. It has been less than a decade since the technology has progressed sufficiently to make this possible. The appropriate signatures may well change as our perceptions and concepts are refined.

ACKNOWLEDGMENTS

Discussions with Lee Hartmann, Scott Kenyon, and George Withbroe are gratefully acknowledged. Dieter Reimers commented thoughtfully on the manuscript. Thanks to Stephanie Deeley for tracking down references and producing an error-free typescript. This review was partially supported by NASA Grant NAGW-511 to the Smithsonian Astrophysical Observatory.

Literature Cited

Aaronson, M., Mould, J. 1982. *Ap. J. Suppl.* 48: 161–84
Aaronson, M., Mould, J. 1985. *Ap. J.* 288: 551–57
Adams, W. S., MacCormack, E. 1935. *Ap. J.* 81: 119–31
Allen, C. W. 1973. *Astrophysical Quantities*, p. 209. London/New York: Athlone Press, Oxford Univ. Press
Athay, R. G., Gurman, J. B., Henze, W. 1983. *Ap. J.* 269: 706–14
Avrett, E. H. 1981. In *Solar Phenomena in Stars and Stellar Systems*, ed. R. M. Bonnet, A. K. Dupree, pp. 173–98. Boston: Reidel
Avrett, E. H., Vernazza, J. E., Linsky, J. L. 1976. *Ap. J. Lett.* 207: L199–204
Ayres, T. R. 1984. *Ap. J.* 284: 784–98
Ayres, T., Linsky, J. L. 1975. *Ap. J.* 200: 660–74
Ayres, T. R., Linsky, J. L., Vaiana, G. S., Golub, L., Rosner, R. 1981. *Ap. J.* 250: 293–99
Ayres, T. R., Simon, T., Linsky, J. L. 1982. *Ap. J.* 263: 791–802
Baliunas, S. L., Avrett, E. H., Hartmann, L., Dupree, A. K. 1979. *Ap. J. Lett.* 233: L129–33
Baliunas, S., Dupree, A. K. 1979. *Ap. J.* 227: 870–83
Baliunas, S., Dupree, A. K. 1982. *Ap. J.* 252: 668–80
Baliunas, S., Hartmann, L., Dupree, A. K. 1983. *Ap. J.* 271: 672–80
Bernat, A. P. 1977. *Ap. J.* 213: 756–66
Bernat, A. P. 1982. *Ap. J.* 252: 644–52
Bernat, A. P., Lambert, D. L. 1976. *Ap. J.* 204: 830–37
Bloemhof, E., Danchi, W. C., Townes, C. H. 1985. *Ap. J. Lett.* 299: L37–40
Boesgaard, A. M. 1979. *Ap. J.* 232: 485–95
Boesgaard, A. M., Hagen, W. 1979. *Ap. J.* 231: 128–38
Bohlin, J. D. 1977. In *Coronal Holes and High Speed Wind Streams*, ed. J. B. Zirker, pp. 27–69. Boulder: Colo. Assoc. Univ. Press
Böhm-Vitense, E. 1981. *Ap. J.* 244: 504–10
Bowers, P. F., Johnston, K. J., Spencer, J. H. 1983. *Ap. J.* 274: 733–54
Breneman, H. H., Stone, E. C. 1985. *Ap. J. Lett.* 299: L57–61
Brosius, J. W., Mullan, D. J. 1986. *Ap. J.* 301: 650–63
Brosius, J. W., Mullan, D. J., Stencel, R. E. 1985. *Ap. J.* 288: 310–28
Brown, A. 1986. In *Advances in Space Research, Proc. COSPAR Meet., 26th.* New York: Pergamon. In press
Brown, A., Jordan, C., Stencel, R. E., Linsky, J. L., Ayres, T. R. 1984. *Ap. J.* 283: 731–44
Brueckner, G. E., Bartoe, J. D. F. 1983. *Ap. J.* 272: 329–48
Brueckner, G. E., Bartoe, J. D. F., Van Hoosier, M. E. 1977. *Proc. OSO-8 Workshop*, pp. 380–418. Boulder: Univ. Colo.
Burlaga, L. F. 1983. *J. Geophys. Res.* 88: 6085–94
Burlaga, L. F. 1984. *Space Sci. Rev.* 39: 255–316
Cacciari, C., Freeman, K. C. 1983. *Ap. J.* 268: 185–94
Carpenter, K. G. 1984. *Ap. J.* 285: 181–89

Carpenter, K. G., Brown, A., Stencel, R. E. 1985. *Ap. J.* 289: 676–80
Cassinelli, J. P. 1979. *Ann. Rev. Astron. Astrophys.* 17: 275–308
Castellani, V., Chieffi, A., Pulone, L., Tornambe, A. 1985. *Ap. J. Lett.* 294: L31–33
Castellani, V., Renzini, A. 1968. *Astrophys. Space Sci.* 2: 310–14
Che, A., Hempe, K., Reimers, D. 1983. *Astron. Astrophys.* 126: 225–39
Che, A., Reimers, D. 1983. *Astron. Astrophys.* 127: 227–30
Chiu, H. Y., Adams, P. S., Linsky, J. L., Basri, G. S., Maran, S. P., Hobbs, R. W. 1977. *Ap. J.* 211: 453–62
Cohen, J. 1976. *Ap. J. Lett.* 203: L127–29
Conti, P. S. 1978. *Ann. Rev. Astron. Astrophys.* 16: 371–92
Cook, W. R., Stone, E. C., Vogt, R. E. 1980. *Ap. J. Lett.* 238: L97–101
Cushman, G. W., Rense, W. A. 1976. *Ap. J. Lett.* 207: L61–62
Cushman, G. W., Rense, W. A. 1977. *Ap. J. Lett.* 211: L57
De Campli, W., Baliunas, S. L. 1979. *Ap. J.* 230: 815–21
de Jong, T. 1983. *Ap. J.* 274: 252–60
Dere, K. P. 1983. In *Solar Wind Five, NASA CP-2280*, ed. M. Neugebauer, pp. 33–43
Dere, K. P., Bartoe, J. D. F., Brueckner, G. E. 1984. *Ap. J.* 281: 870–83
Deutsch, A. J. 1956. *Ap. J.* 123: 210–27
Drake, S. A., Brown, A., Linsky, J. 1984. *Ap. J.* 284: 774–83
Drake, S. A., Linsky, J. L. 1983a. *Ap. J.* 273: 299–308
Drake, S. A., Linsky, J. L. 1983b. *Ap. J. Lett.* 274: L77–81
Drake, S. A., Linsky, J. L. 1984. *Proc. Cambridge Workshop Cool Stars, Stellar Systems, and the Sun, 3rd*, ed. S. L. Baliunas, L. Hartmann, pp. 350–52. New York: Springer-Verlag
Dupree, A. K. 1975. *Ap. J. Lett.* 200: L27–31
Dupree, A. K. 1976. In *Physiques des Mouvements dans les Atmosphères Stellaires, Int. CNRS No. 250*, ed. R. Cayrel, M. Steinberg, pp. 439–51
Dupree, A. K. 1981. In *Effects of Mass Loss on Stellar Evolution*, ed. C. Chiosi, R. Stalio, pp. 87–110. Boston: Reidel
Dupree, A. K. 1982. In *Advances in Ultraviolet Astronomy: Four Years of IUE Research, NASA CP-2238*, ed. Y. Kondo, J. Mead, R. Chapman, pp. 3–16
Dupree, A. K., Baliunas, S. L. 1979. *IAU Circ. No. 3435*
Dupree, A. K., Baliunas, S. L., Guinan, E. F., Hartmann, L., Sonneborn, G. S. 1986. *Proc. Cambridge Workshop Cool Stars, Stellar Systems, and the Sun, 4th*, ed. D. Gibson, M. Zeilik. New York: Springer-Verlag. In press
Dupree, A. K., Hartmann, L., Avrett, E. H. 1984a. *Ap. J. Lett.* 281: L37–39
Dupree, A. K., Hartmann, L., Smith, G. 1984b. *Proc. Cambridge Workshop Cool Stars, Stellar Systems, and the Sun, 3rd*, ed. S. L. Baliunas, L. Hartmann, pp. 326–29. New York: Springer-Verlag
Dupree, A. K., Sonneborn, G., Baliunas, S. L., Guinan, E. F., Hartmann, L. 1984c. In *Future of Ultraviolet Astronomy Based on Six Years of IUE Research, NASA CP-2349*, ed. J. M. Mead, R. D. Chapman, Y. Kondo, pp. 462–67
Flower, P. J. 1977. *Astron. Astrophys.* 54: 31–39
Frogel, J. A., Persson, S. E., Cohen, J. G. 1981. *Ap. J.* 246: 842–65
Fusi-Pecci, F., Renzini, A. 1978. In *IAU Symp. No. 80*, ed. A. G. D. Philip, D. S. Hayes, pp. 225–28. Boston: Reidel
Gehrz, R. D., Woolf, N. J. 1971. *Ap. J.* 165: 285–94
Geiss, J. 1982. *Space Sci. Rev.* 33: 201–17
Geiss, J., Bochsler, P. 1984. *Proc. Int. Conf. Isotopic Ratios in the Solar System, Paris.* In press
Goldberg, L. 1979. *Q. J. R. Astron. Soc.* 20: 361–82
Goldberg, L. 1985. *CNRS-NASA Monogr. Ser. Nonthermal Phenomena in Stellar Atmospheres, the M, S, and C Stars.* In press
Gosling, J. T., Borrini, G., Asbridge, J. R., Bame, S. J., Feldman, W. C., Hansen, R. T. 1981. *J. Geophys. Res.* 86(A7): 5438–48
Gosling, J. T., Hundhausen, A., Bame, S. J. 1976. *J. Geophys. Res.* 81: 2111–22
Gouttebroze, P., Leibacher, J. W. 1980. *Ap. J.* 238: 1134–51
Gratton, R. 1983. *Ap. J.* 264: 223–27
Gratton, R. G., Pilachowski, C. A., Sneden, C. 1984. *Astron. Astrophys.* 132: 11–19
Guinan, E. F. 1984. *Proc. Cambridge Workshop Cool Stars, Stellar Systems, and the Sun, 3rd*, ed. S. L. Baliunas, L. Hartmann, pp. 336–41. New York: Springer-Verlag
Gurman, J. B., Athay, R. G. 1983. *Ap. J.* 273: 374–80
Hagen, H. J. 1984. Diplomarbeit. Univ. Hamburg, West Germ.
Hagen, W. 1978. *Ap. J. Suppl.* 38: 1–18
Hagen, W. 1980. In *Cool Stars, Stellar Systems, and the Sun, SAO Spec. Rep. No. 389*, ed. A. K. Dupree, pp. 143–52
Hagen, W. 1982. *Publ. Astron. Soc. Pac.* 94: 835–44
Hagen, W., Stencel, R. E., Dickinson, D. F. 1983. *Ap. J.* 274: 286–301
Hall, D. S. 1972. *Publ. Astron. Soc. Pac.* 84: 323–33
Hall, D. S. 1976. In *Multiple Periodic Vari-*

able Stars, IAU Colloq. No. 29, ed. W. S. Fitch, p. 287. Boston: Reidel
Hartmann, L., Avrett, E. H. 1984. *Ap. J.* 284: 238–49
Hartmann, L., Dupree, A. K., Raymond, J. C. 1980. *Ap. J. Lett.* 236: L143–47
Hartmann, L., Dupree, A. K., Raymond, J. C. 1981. *Ap. J.* 246: 193–202
Hartmann, L., Dupree, A. K., Raymond, J. C. 1982. *Ap. J.* 252: 214–29
Hartmann, L., Jordan, C., Brown, A., Dupree, A. K. 1985. *Ap. J.* 296: 576–92
Hartmann, L., MacGregor, K. B. 1980. *Ap. J.* 242: 260–82
Harvey, J. W., Sheeley, N. R. Jr. 1977. *Sol. Phys.* 54: 343–51
Heasley, J. N. 1975. *Sol. Phys.* 44: 275–92
Helfand, D. J., Caillault, J. P. 1982. *Ap. J.* 253: 760–67
Hempe, K. 1982. *Astron. Astrophys.* 115: 133–37
Hempe, K. 1984. *Astron. Astrophys. Suppl.* 56: 115–67
Hjellming, R. M., Newell, R. T. 1983. *Ap. J.* 275: 704–8
Hoffleit, D. 1982. *The Bright Star Catalogue*. New Haven, Conn: Yale Univ. Obs.
Holzer, T. E., Fla, T., Leer, E. 1983. *Ap. J.* 275: 808–35
Holzer, T. E., MacGregor, K. B. 1985. In *Mass Loss from Red Giants*, ed. M. Morris, B. Zuckerman, pp. 229–55. Boston: Reidel
Howard, R. A., Sheeley, N. R., Koomen, M. J., Michels, D. J. 1985. *J. Geophys. Res.* 90(A9): 8173–91
Huber, M. C. E., Foukal, P. V., Noyes, R. W., Reeves, E. M. 1974. *Ap. J. Lett.* 194: L115–18
Hummer, D. G., Rybicki, G. B. 1968. *Ap. J. Lett.* 153: L107–10
Hundhausen, A. J. 1985. In *Collisionless Shocks in the Heliosphere: A Tutorial Review, Geophys. Monogr.*, ed. R. G. Stone, B. T. Tsurutani, 34: 37–58. Washington, DC: Am. Geophys. Union
Iben, I. Jr., Renzini, A. 1983. *Ann. Rev. Astron. Astrophys.* 21: 271–342
Iben, I. Jr., Rood, R. T. 1970. *Ap. J.* 161: 587–617
Jura, M. 1986. *Irish Astron. J.* In press
Jura, M., Morris, M. 1981. *Ap. J.* 251: 181–89
Karovska, M., Nisenson, P., Noyes, R. W., Roddier, F. 1986. *Ap. J.* 308: In press
Kenyon, S. J. 1986. *The Symbiotic Stars*. Cambridge: Cambridge Univ. Press. In press
Kenyon, S. J., Webbink, R. F. 1984. *Ap. J.* 279: 252–83
Knapp, G. R., Bowers, P. F. 1983. *Ap. J.* 266: 701–12
Knapp, G. R., Morris, M. 1985. *Ap. J.* 292: 640–69
Knapp, G. R., Phillips, T. G., Huggins, P. J. 1980. *Ap. J. Lett.* 242: L25–28
Knapp, G. R., Phillips, T. G., Leighton, R. B., Lo, K. Y., Wannier, P. G., et al. 1982. *Ap. J.* 252: 616–34
Kneer, F., Scharmer, G., Mattig, W., Wyller, A., Artzner, G., et al. 1981. *Sol. Phys.* 69: 289–300
Kohl, J. L., Withbroe, G. L., Zapata, C. A., Noci, G. 1983. In *Solar Wind Five, NASA CP-2280*, ed. M. Neugebauer, pp. 47–60
Krieger, A. S., Timothy, A. F., Roelof, E. C. 1973. *Sol. Phys.* 29: 505–25
Kudritzki, R. P., Reimers, D. 1978. *Astron. Astrophys.* 70: 227–39
Kunasz, P. 1973. PhD thesis. Univ. Colo., Boulder
Kunasz, P. B., Morrison, N. D. 1982. *Ap. J.* 263: 226–38
Kunasz, P. B., Morrison, N. D., Spressart, B. 1983. *Ap. J.* 266: 739–46
Lada, C. J. 1985. *Ann. Rev. Astron. Astrophys.* 23: 267–317
Lambert, D. L., Hinkle, K. H., Hall, D. N. B. 1981. *Ap. J.* 248: 638–50
Linsky, J. L., Haisch, B. M. 1979. *Ap. J. Lett.* 229: L27–32
Linsky, J. L., Hunten, D. M., Sowell, R., Glackin, D. L., Kelch, W. L. 1979b. *Ap. J. Suppl.* 41: 481–500
Linsky, J. L., Worden, S. P., McClintock, W., Robertson, R. M. 1979a. *Ap. J. Suppl.* 41: 47–74
Lites, B. W., Skumanich, A. 1982. *Ap. J. Suppl.* 49: 293–316
Luck, R. E., Lambert, D. L. 1982. *Ap. J.* 256: 189–205
MacGregor, K. B. 1983. In *Solar Wind Five, NASA CP-2280*, ed. M. Neugebauer, pp. 241–61
Maeder, A., Mermilliod, J. C. 1981. *Astron. Astrophys.* 93: 136–49
Mallia, E. A., Pagel, B. E. J. 1978. *MNRAS* 184: 55p–59p
Mallik, S. V. 1982. *J. Astrophys. Astron.* 3: 39–61
Mariska, J. T. 1980. *Ap. J.* 235: 268–73
Mauron, N., Fort, B., Querci, F., Dreux, M., Fauconnier, T., Lamy, P. 1984. *Astron. Astrophys.* 130: 341–47
Mauron, N., Cailloux, M., Prieur, J. L., Tilloles, P., Le Fèvré, O. 1986. *Astron. Astrophys.* In press
Mewaldt, R. A. 1980. *Proc. Conf. Ancient Sun*, ed. R. O. Pepin, J. A. Eddy, R. B. Merrill, pp. 81–101. New York: Pergamon
Meyer, J. P. 1985a. *Ap. J. Suppl.* 57: 151–71
Meyer, J. P. 1985b. *Ap. J. Suppl.* 57: 173–204

Milkey, R. W., Heasley, J. N., Beebe, H. A. 1973. *Ap. J.* 186: 1043–52
Mould, J., Aaronson, M. 1982. *Ap. J.* 263: 629–38
Mullan, D. J. 1978. *Ap. J.* 226: 151–66
Mullan, D. J. 1984a. *Ap. J.* 283: 303–12
Mullan, D. J. 1984b. *Ap. J.* 284: 769–73
Mullan, D. J., Stencel, R. E. 1982. *Ap. J.* 253: 716–26
Neugebauer, M. 1983. In *Solar Wind Five, NASA CP-2280*, ed. M. Neugebauer, pp. 135–45
Newell, R. T., Hjellming, R. M. 1982. *Ap. J. Lett.* 263: L85–87
Noerdlinger, P. D., Rybicki, G. B. 1974. *Ap. J.* 193: 651–76
O'Brien, G. T. Jr. 1980. *A study of the 10830 Å line of neutral helium in the spectra of red giants*. PhD thesis. Univ. Texas, Austin
Olnon, F. M. 1975. *Astron. Astrophys.* 39: 217–23
Oranje, B. J. 1983. *Astron. Astrophys.* 122: 88–94
Orrall, F. Q., Rottman, G. J., Klimchuk, J. A. 1983. *Ap. J. Lett.* 266: L65–68
Paczynski, B., Rudak, B. 1980. *Astron. Astrophys.* 82: 349–51
Paczynski, B., Ziolkowski, J. 1968a. *Acta Astron.* 18: 255–66
Paczynski, B., Ziolkowski, J. 1968b. In *IAU Symp. No. 34*, ed. D. E. Osterbrock, C. R. O'Dell, pp. 396–99. Dordrecht/Boston: Reidel
Panagia, N., Felli, M. 1975. *Astron. Astrophys.* 39: 1–5
Parker, E. N. 1963. *Interplanetary Dynamical Processes*. New York: Interscience. 272 pp.
Peterson, R. C. 1981. *Ap. J. Lett.* 248: L31–34
Peterson, R. C. 1982. *Ap. J.* 258: 499–505
Peterson, R. C. 1983. *Ap. J.* 275: 737–51
Peterson, R. C. 1985. *Ap. J.* 289: 320–25
Pizzo, V. 1985. In *Collisionless Shocks in the Heliosphere: Reviews of Current Research, Geophys. Monogr.*, ed. R. G. Stone, T. Tsurutani, 34: 51–68. Washington, DC: Am. Geophys. Union
Popper D. M., Ulrich, R. K. 1977. *Ap. J. Lett.* 212: L131–34
Pylyser, E., Doom, C., deLoore, C. 1985. *Astron. Astrophys.* 148: 379–85
Ramsey, L. W. 1979. *Publ. Astron. Soc. Pac.* 91: 252–54
Reid, N., Mould, J. R. 1984. *Ap. J.* 284: 98–107
Reimers, D. 1975a. In *Problems in Stellar Atmospheres and Envelopes*, ed. B. Baschek, W. H. Hegel, G. Traving, pp. 229–256. New York: Springer-Verlag
Reimers, D. 1975b. *Mem. Soc. R. Sci. Liège, 6e Ser.* 8: 369–82
Reimers, D. 1977a. *Astron. Astrophys.* 57: 395–400
Reimers, D. 1977b. *Astron. Astrophys.* 61: 217–24
Reimers, D. 1978. *Astron. Astrophys.* 67: 161
Reimers, D. 1981. In *Physical Processes in Red Giants*, ed. I. Iben Jr., A. Renzini, pp. 269–84. Dordrecht/Boston: Reidel
Reimers, D. 1982. *Astron. Astrophys.* 107: 292–99
Reimers, D. 1984. *Astron. Astrophys.* 136: L5–6
Reimers, D. 1986. *Astron. Astrophys.* In press
Reimers, D., Che-Bohenstengel, A. 1986. *Astron. Astrophys.* In press
Reimers, D., Schröder, K. P. 1983. *Astron. Astrophys.* 124: 241–46
Renzini, A. 1981. In *Physical Processes in Red Giants*, ed. I. Iben Jr., A. Renzini, pp. 431–46. Dordrecht/Boston: Reidel
Renzini, A., Bernazzani, M., Buonanno, R., Corsi, C. E. 1985. *Ap. J. Lett.* 294: L7–11
Ridgway, S. T., Joyce, R. R., White, N. M., Wing, R. F. 1980. *Ap. J.* 235: 126–37
Rood, R. T. 1973. *Ap. J.* 184: 815–37
Rottman, G. J., Orrall, F. Q. 1983. In *Solar Wind Five, NASA CP-2280*, ed. M. Neugebauer, pp. 199–210
Rottman, G. J., Orrall, F. Q., Klimchuk, J. A. 1982. *Ap. J.* 260: 326–37
Sanner, F. 1976. *Ap. J. Suppl.* 32: 115–45
Schröder, K. P. 1985. *Astron. Astrophys.* 147: 103–10
Shine, R. A. 1975. *Ap. J.* 202: 543–50
Simon, T., Linsky, J. L., Stencel, R. E. 1982. *Ap. J.* 257: 225–46
Smith, G. H., Dupree, A. K. 1986. Submitted for publication
Sopka, R. J., Hildebrand, R., Jaffe, D. T., Gatley, I., Roellig, T., et al. 1985. *Ap. J.* 294: 242–55
Sparks, W. M., Kutter, G. S. 1972. *Ap. J.* 175: 707–15
Spergel, D. N., Giuliani, J. L. Jr., Knapp, G. R. 1983. *Ap. J.* 275: 330–41
Spite, M., Caloi, V., Spite, F. 1981. *Astron. Astrophys.* 103: L11–13
Sreenivasan, S. R., Wilson, W. J. F. 1985. *Ap. J.* 290: 653–59
Stencel, R. E. 1978. *Ap. J. Lett.* 223: L37–39
Stencel, R. E., Mullan, D. J. 1980a. *Ap. J.* 238: 221–28
Stencel, R. E., Mullan, D. J. 1980b. *Ap. J.* 240: 718
Tuchman, Y., Sack, N., Barkat, Z. 1979. *Ap. J.* 234: 217–27
Tutukov, A. V., Yungelson, L. R. 1982. In *The Nature of Symbiotic Stars, IAU Colloq. No. 70*, ed. M. Freidjung, R. Viotti, pp. 283–96. Dordrecht: Reidel

Vaiana, G. S., Cassinelli, J. P., Fabbiano, G., Giacconi, R., Golub, L., et al. 1981. *Ap. J.* 245: 163–82
van der Hucht, K. A., Bernat, A. P., Kondo, Y. 1980. *Astron. Astrophys.* 82: 14–29
Vaughan, A. H. Jr. 1968. *Ap. J.* 154: 87–101
Veck, N. J., Parkinson, J. H. 1981. *MNRAS* 197: 41–55
Vernazza, J. E., Avrett, E. H., Loeser, R. 1981. *Ap. J. Suppl.* 45: 635–725
Wagner, W. J. 1984. *Ann. Rev. Astron. Astrophys.* 22: 267–89
Walker, M. F. 1955. *Astron. J.* 60: 197
Walter, F. M., Bowyer, S. 1981. *Ap. J.* 245: 671–76
Weiler, E. J. 1978. *Astron. J.* 83: 795–815
Weiler, E. J., Owen, F. N., Bopp, B. W., Schmitz, M., Hall, D. S. 1978. *Ap. J.* 225: 919–31
Welty, D. E. 1985. *Astron. J.* 90: 2555
Weymann, R. 1963. *Ann. Rev. Astron. Astrophys.* 1: 97–144
White, O. R., Livingston, W. C. 1978. *Ap. J.* 226: 679–86
Willson, L. A., Bowen, G. H. 1984. *Nature* 312: 429–31
Withbroe, G. L., Kohl, J. L., Weiser, H., Munro, R. H. 1982. *Space Sci. Rev.* 33: 17–52
Withbroe, G. L., Noyes, R. W. 1977. *Ann. Rev. Astron. Astrophys.* 15: 363–87
Wood, P. R. 1979. *Ap. J.* 227: 220–31
Wood, P. R. 1981. In *Physical Processes in Red Giants*, ed. I. Iben Jr., A. Renzini, pp. 205–23. Dordrecht/Boston: Reidel
Wood, P. R., Cahn, J. H. 1977. *Ap. J.* 211: 499–508
Wright, A. E., Barlow, M. J. 1975. *MNRAS* 170: 41–51
Zarro, D. M., Rodgers, A. W. 1983. *Ap. J. Suppl.* 53: 815–68
Zirin, H. 1976. *Ap. J.* 208: 414–25
Zirker, J. B. 1977. In *Coronal Holes and High Speed Wind Streams*, ed. J. B. Zirker, pp. 4–26. Boulder: Colo. Assoc. Univ. Press
Zirker, J. B. 1981. In *Solar Phenomena in Stars and Stellar Systems*, ed. R. M. Bonnet, A. K. Dupree, pp. 301–18. Boston: Reidel
Zuckerman, B. 1980. *Ann. Rev. Astron. Astrophys.* 18: 263–88